Deep Inelastic Neutron Scattering

The high-energy side of neutron scattering

Roberto Senesi
Università degli Studi di Roma "Tor Vergata", Dipartimento di Fisica and Centro NAST
CNR- IPCF Sezione di Messina
Associazione School of Neutron Scattering "Francesco Paolo Ricci "

Erice School "NEUTRON SCIENCE AND INSTRUMENTATION": DESIGNING AND BUILDING A NEUTRON INSTRUMENT

Neutron spectrum from a water moderator at a Spallation source: 88% of neutrons have energies above 0.4 eV!

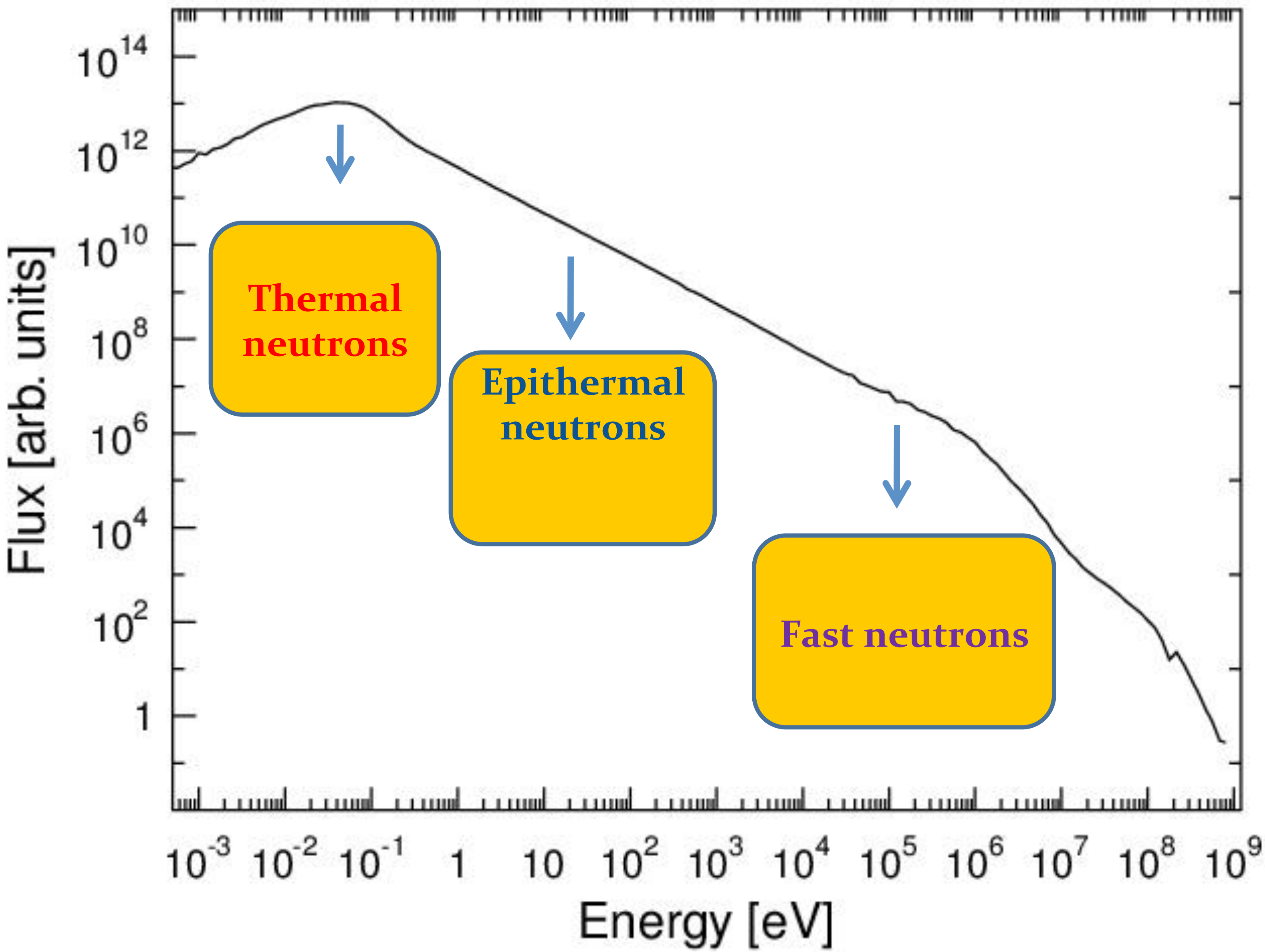

Neutron spectrum from a water moderator
Spallation source: 88% of neutrons have energies above 0.4 eV!

Energy [eV]	Wave length [Å]
0.4	0.45
1	0.29
10	0.09
20	0.06
50	0.04
100	0.03

Which energy and length scales can be probed?

Which energy and length scales can be probed?

Collective and single-particle excitations

Energy [eV]	Wave length [Å]
0.4	0.45
1	0.29
10	0.09
20	0.06
50	0.04
100	0.03

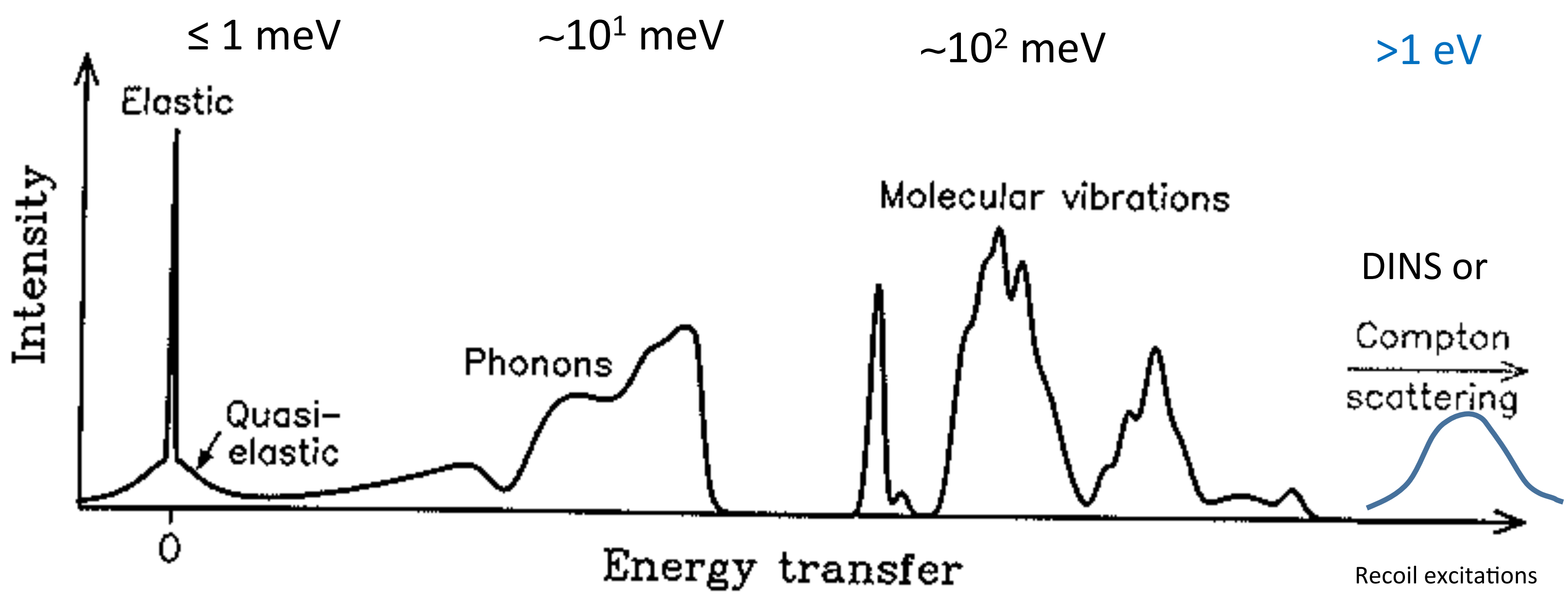

From: "Elementary Scattering Theory For X-ray and Neutron Users" D.S. Sivia OUP (2011)

Does this wave length range match with atomic binding scales ?

Energy [eV]	Wave length [Å]
0.4	0.45
1	0.29
10	0.09
20	0.06
50	0.04
100	0.03

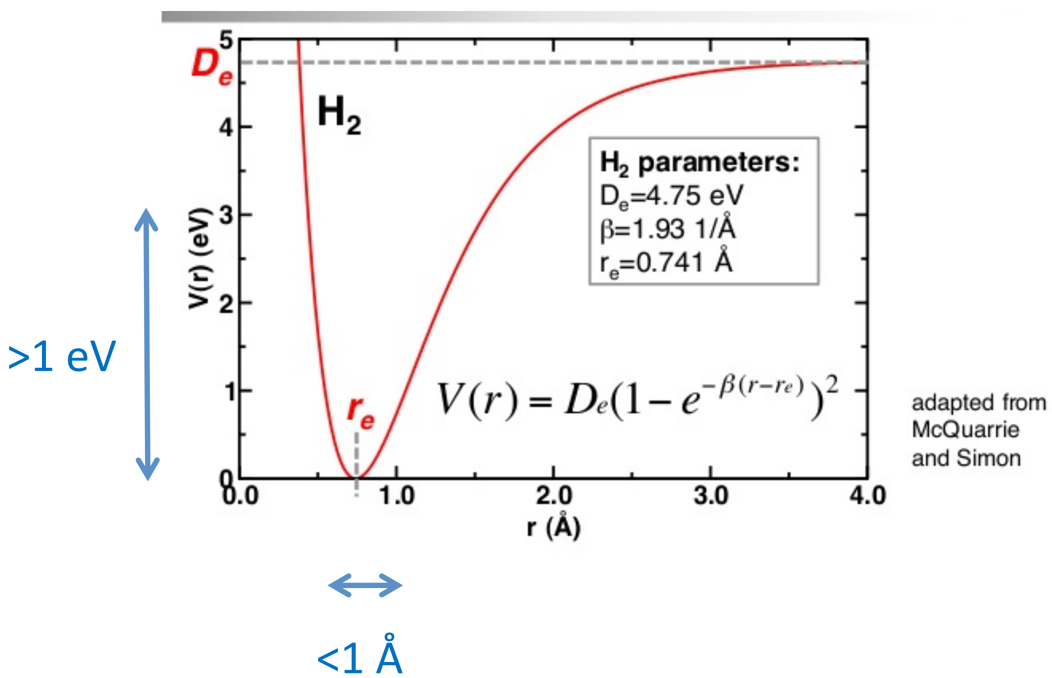

H-H binding (Morse potential) in the H_2 molecule

Wave length range match with atomic binding scales

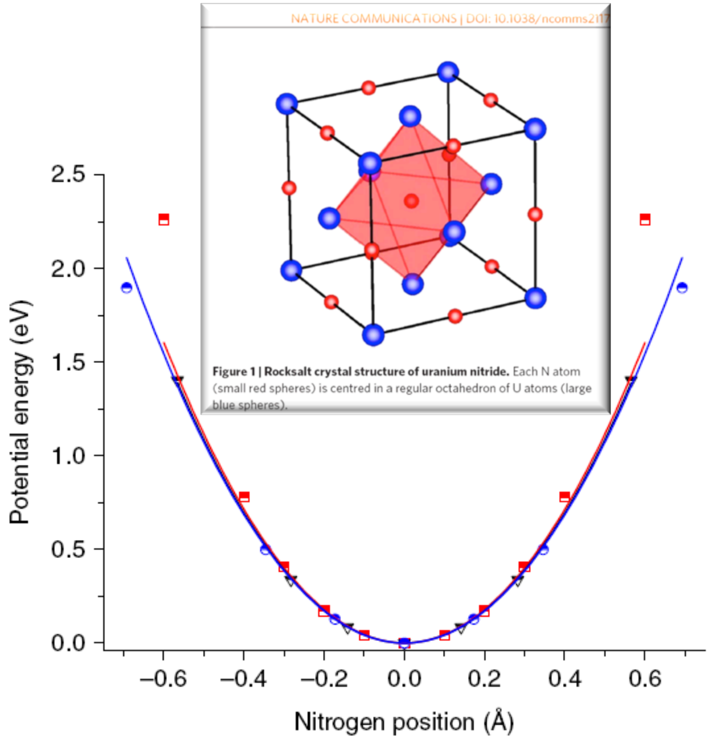

Figure 5 | DFT calculated potential energy of the N atoms in the system UN. The potential energy is shown for atomic displacements relative to the equilibrium position along the [100] (red squares), [110] (black triangles) and [111] (blue circles) directions. The solid lines are fits of the calculated small displacement limit values to parabolic (that is harmonic) potentials. The potential energy is very isotropic and harmonic over a wide range. Deviations are visible above 1 eV, especially along the [100] direction.

Received 6 Jun 2012 | Accepted 4 Sep 2012 | Published 9 Oct 2012 DOI: 10.1038/ncomms2117

Quantum oscillations of nitrogen atoms in uranium nitride

A.A. Aczel[1], G.E. Granroth[1], G.J. MacDougall[1], W.J.L. Buyers[2], D.L. Abernathy[1], G.D. Samolyuk[3], G.M. Stocks[3] & S.E. Nagler[1,4]

Energy [eV]	Wave length [Å]
0.4	0.45
1	0.29
10	0.09
20	0.06
50	0.04
100	0.03

PHYSICAL REVIEW B 83, 220302(R) (2011)

Momentum distribution, vibrational dynamics, and the potential of mean force in ice

Lin Lin,[1] Joseph A. Morrone,[2,*] Roberto Car,[1,2,3,†] and Michele Parrinello[4]

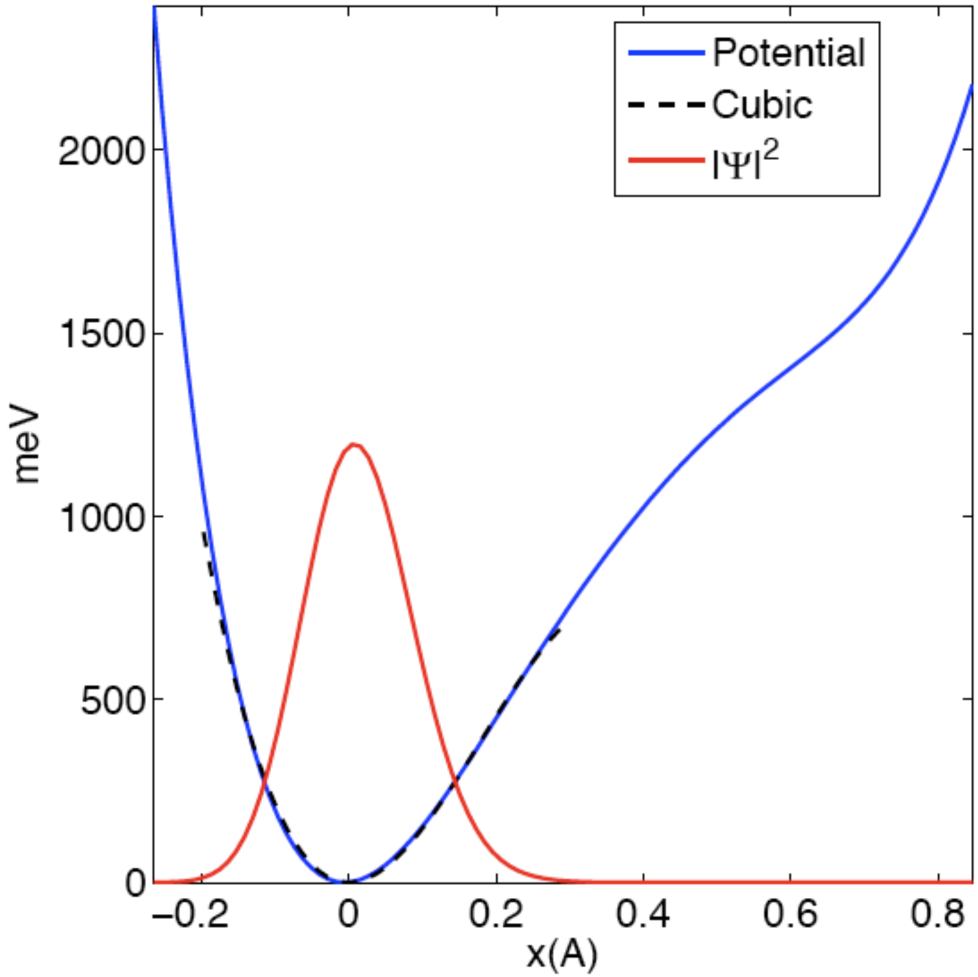

Most energetic vibration in water: stretching!

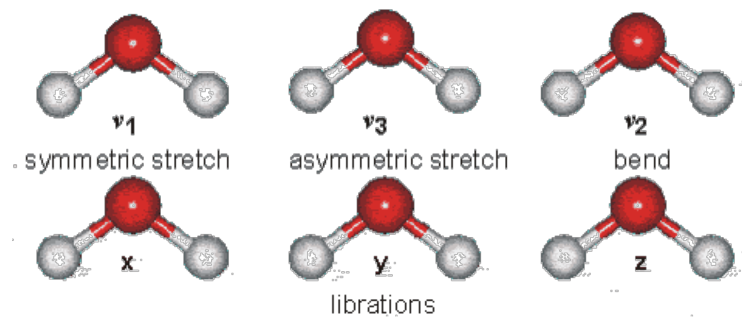

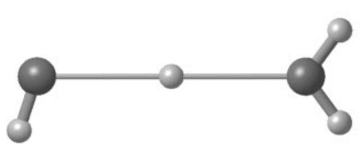

Potential energy surface of the proton along the bond

Mechanical properties of solids and details of atomic binding

Figure 7.5 (a) A pair potential curve and (b) its derivative. The bulk modulus us related to the slope of the first derivative at the point where the slope is zero.

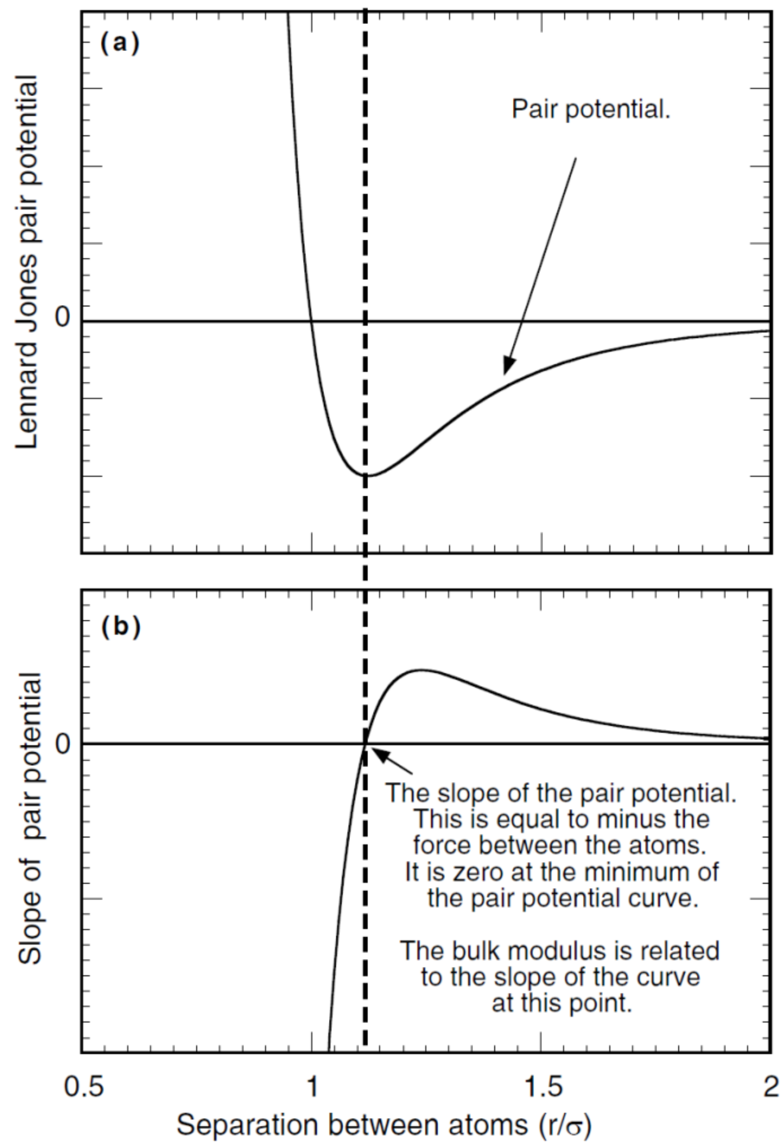

Mechanical properties of solids and details of atomic binding

Figure 7.7 The potential energy of interaction between atoms in a solid. (a) The *harmonic approximation*: How the energy would vary if the atoms were connected by 'perfect springs'. (b) The typical deviation from the harmonic approximation of a real interatomic potential. The sloping line indicates the increasing average separation as the average energy of oscillation (i.e. the temperature) is increased.

(a)

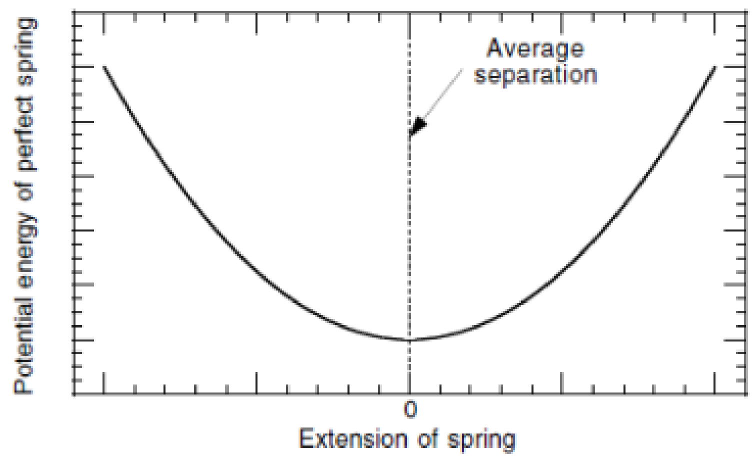

(b)

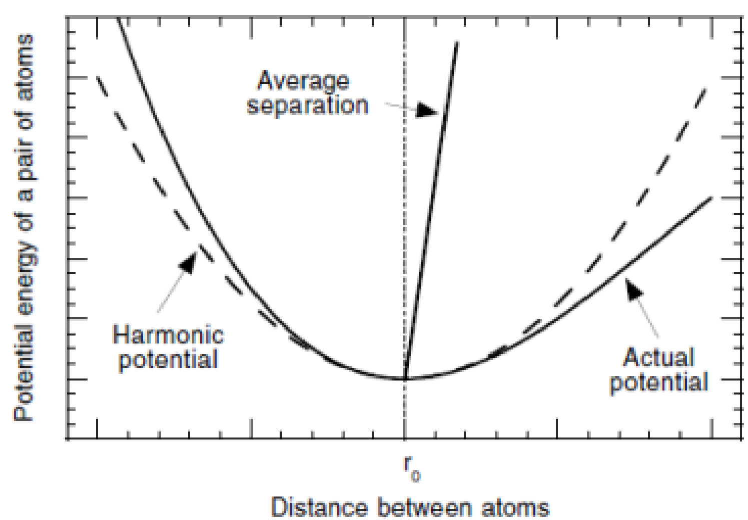

Mechanical properties of solids and details of atomic binding

Figure 7.9 Schematic illustration of the potential energy of an Fe–Ni bond in an invar alloy (Table 7.8). The asymmetry of the potential (over a certain range) is opposite to that which occurs in normal bonds (Figure 7.7).

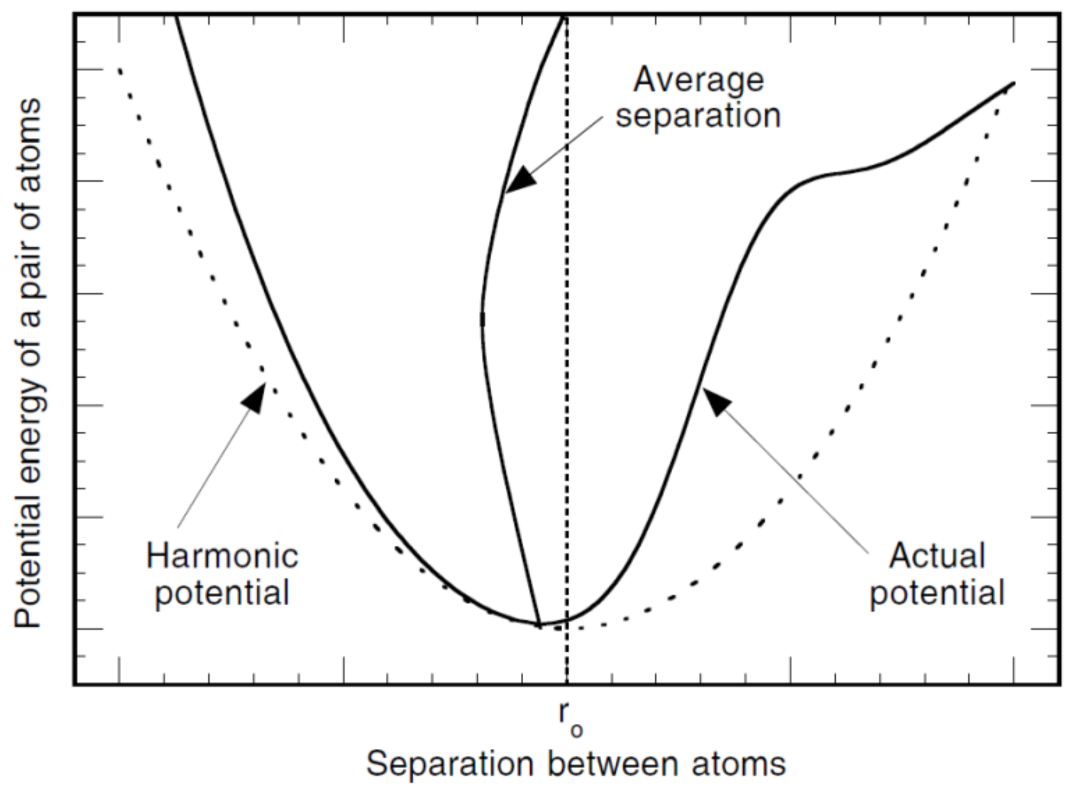

Quantum effects involved!

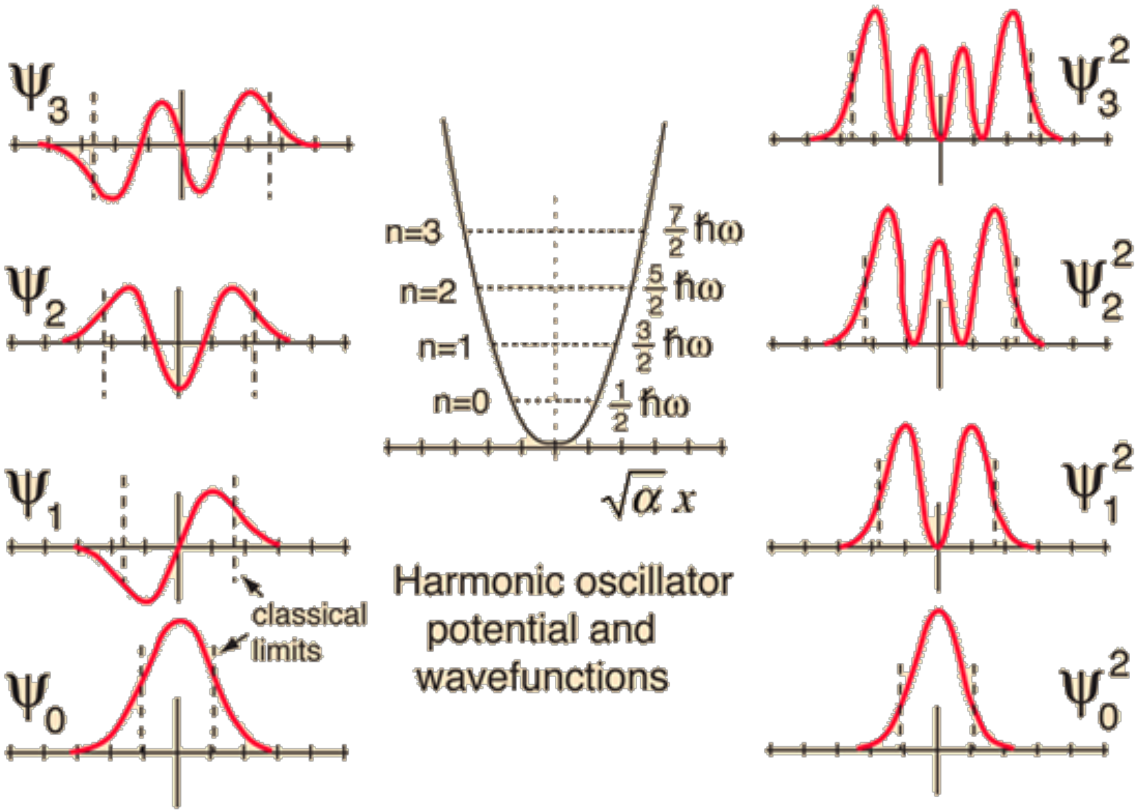

The Fourier Transform of

$$|\Psi|^2 \quad \text{is}$$

$$n(p)$$ Momentum distribution

The variance of $n(p)$ is

$$\langle E_K \rangle = \frac{\langle p^2 \rangle}{2M}$$ Kinetic energy

$$\langle E_K \rangle >> 1.5 k_B T \,!!$$

High energy (eV) neutrons can be used to probe the shapes and depths of potentials Knowledge of potentials is relevant for the description of mechanical, thermal , structural properties of materials!

Measurements of momentum distributions using inelastic neutron scattering

- Can we measure $\Psi(x), \Psi(p)$? No
- Deep Inelastic Neutron Scattering allows to measure $|\Psi(p)|^2$
- Not exactly- DINS can probe $n(p)$
- That is, the distribution (probability density) of atomic (nuclei) momentum being equal to ***p***

The Fourier Transform of $|\Psi|^2$ is $n(p)$ Momentum distribution

The variance of $n(p)$ is

$$\langle E_K \rangle = \frac{\langle p^2 \rangle}{2M}$$ Kinetic energy

$$\langle E_K \rangle >> 1.5 k_B T\,!!$$

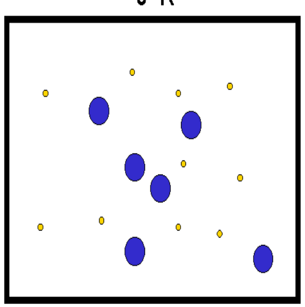

Measurements of momentum distributions using inelastic neutron scattering

A classical analogue: we want to measure the momentum (or velocity) of an atom in the sample (target), which has velocity $\mathbf{v}_{ti}$

A neutron with velocity $\mathbf{v}_{ni}$ is sent to the target and is scattered at an angle θ. The final velocity of the neutron is $\mathbf{v}_{nf}$

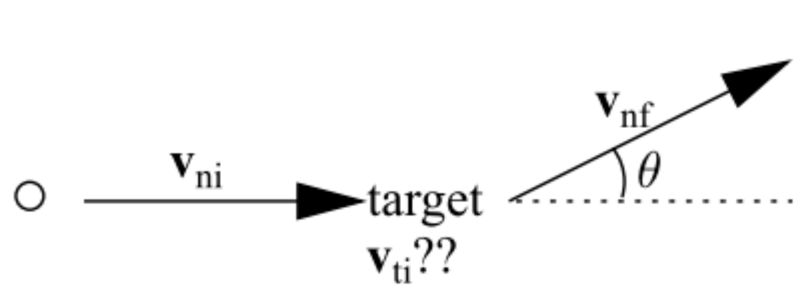

By measuring $\mathbf{v}_{ni}$, θ, $\mathbf{v}_{nf}$ s we can derive $\mathbf{v}_{ti}$

Repeat many times and sample the distribution of $\mathbf{v}_{ti}$ for as many atoms as possible.
Typically we can "send" 10^7 neutrons/(cm^2 s)

0º K

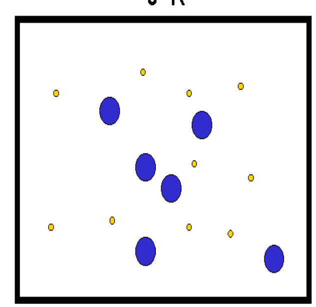

Measurements of momentum distributions using inelastic neutron scattering

A classical analogue: an incident particle m_n and a target particle $m_t = m_n$ with initial velocities $\mathbf{v}_{ni}$ and $\mathbf{v}_{ti}$

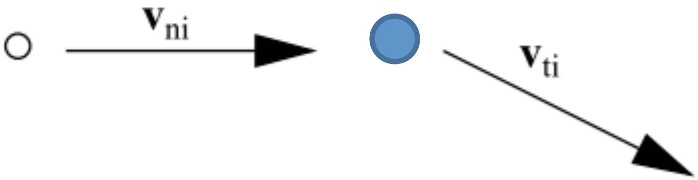

After the scattering m_n has velocity $\mathbf{v}_{nf}$, and we are able to measure only $\mathbf{v}_{ni}$, $\mathbf{v}_{nf}$

Measurements of momentum distributions using inelastic neutron scattering

Apply conservation of momenta and kinetic energy

$$\begin{aligned} m_n = m_t &= m \\ \mathbf{v}_{ni} + \mathbf{v}_{ti} &= \mathbf{v}_{nf} + \mathbf{v}_{tf} \\ v_{ni}^2 + v_{ti}^2 &= v_{nf}^2 + v_{tf}^2 \end{aligned} \tag{1}$$

And defining

$$\begin{aligned} \Delta\mathbf{v} &= \mathbf{v}_{ni} - \mathbf{v}_{nf} \\ \omega &= v_{ni}^2 - v_{nf}^2 \end{aligned} \tag{2}$$

We obtain

$$\begin{aligned} \Delta\mathbf{v} + \mathbf{v}_{ti} &= \mathbf{v}_{tf} \\ v_{ti}^2 + \omega &= v_{tf}^2 \end{aligned} \tag{3}$$

Measurements of momentum distributions using inelastic neutron scattering

Squaring the first equation and substituting into the second

$$v_{tf}^2 = v_{ti}^2 + (\Delta v)^2 - 2\,\Delta\mathbf{v}\cdot\mathbf{v}_{ti} \qquad (4)$$
$$v_{ti}^2 + \omega = v_{ti}^2 + (\Delta v)^2 - 2\,\Delta\mathbf{v}\cdot\mathbf{v}_{ti}$$

we have

$$\omega = (\Delta v)^2 - 2\,\Delta\mathbf{v}\cdot\mathbf{v}_{ti} = (\Delta v)^2 - 2\Delta v\, v_{ti}\cos\theta \qquad (5)$$

where θ is the scattering angle!

Can be generalised to the case $m_t \neq m_n$

In neutron scattering formalism:

$\omega \to$ energy transfer; $\Delta\mathbf{v} \to$ wave vector transfer; $(\Delta v)^2 \to$ recoil energy $\hbar^2 q^2/(2\,m_t)$

Can a neutron scattering instrument put in practice the billiard-ball experiment?

Wave vector and energy transfers using inelastic neutron scattering at eV energies: detector trajectories+proton and deuteron recoil trajectories

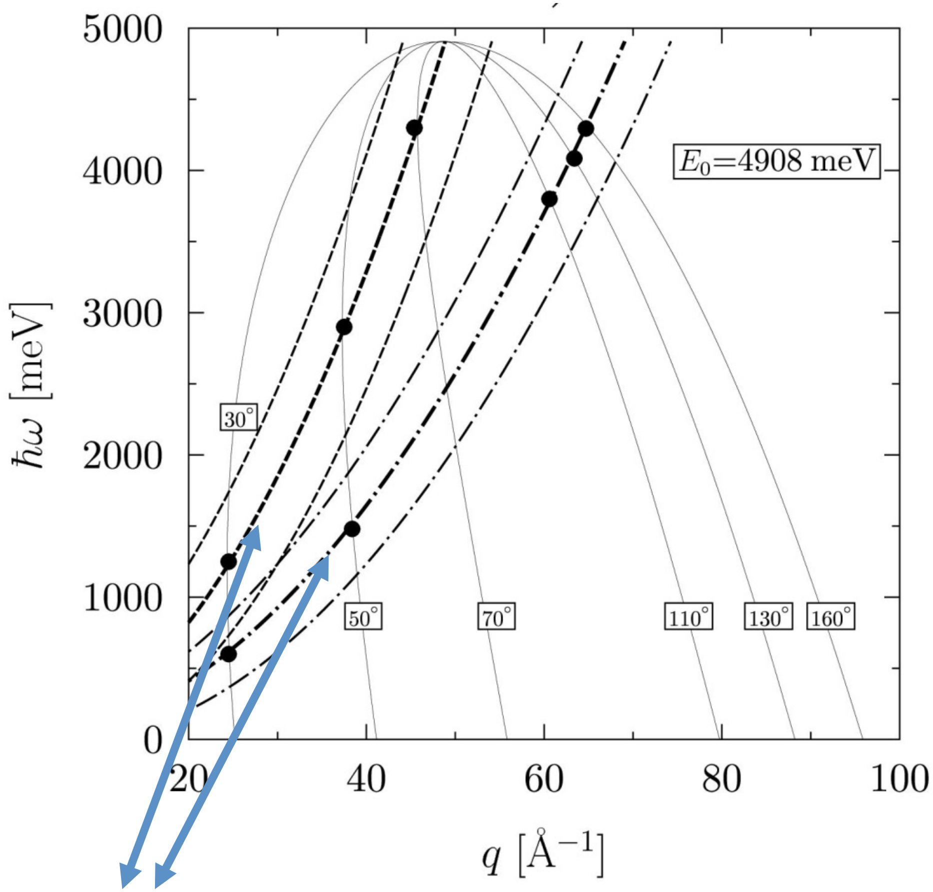

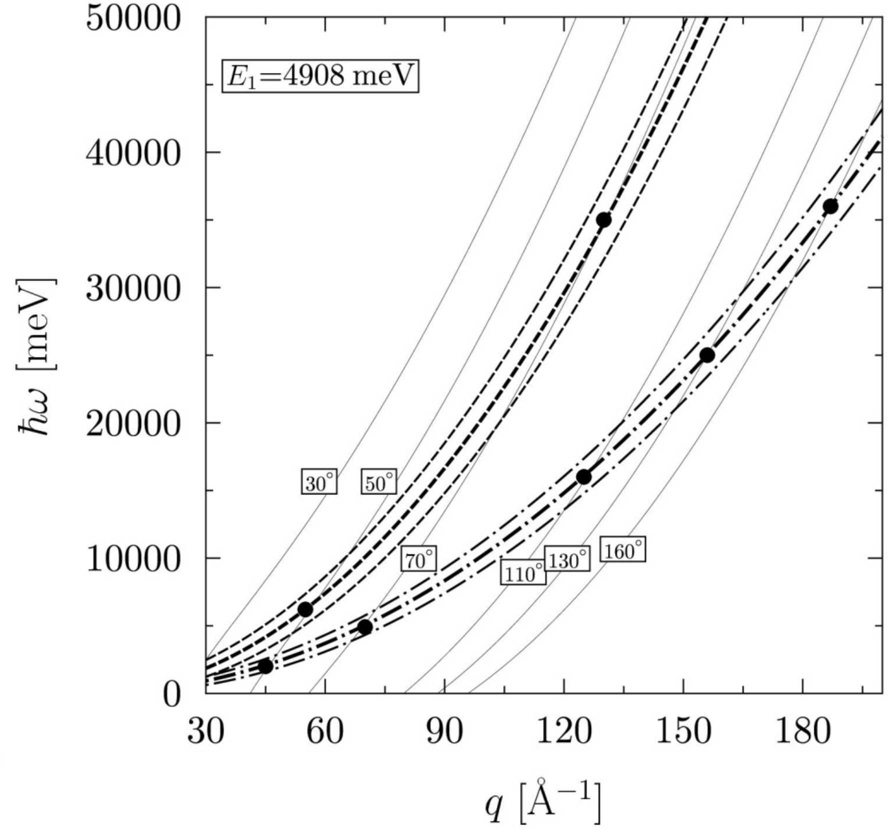

Recoil lines
+
Broadening

Direct geometry

Inverse geometry

Kinematic of scattering in the Impulse Approximation

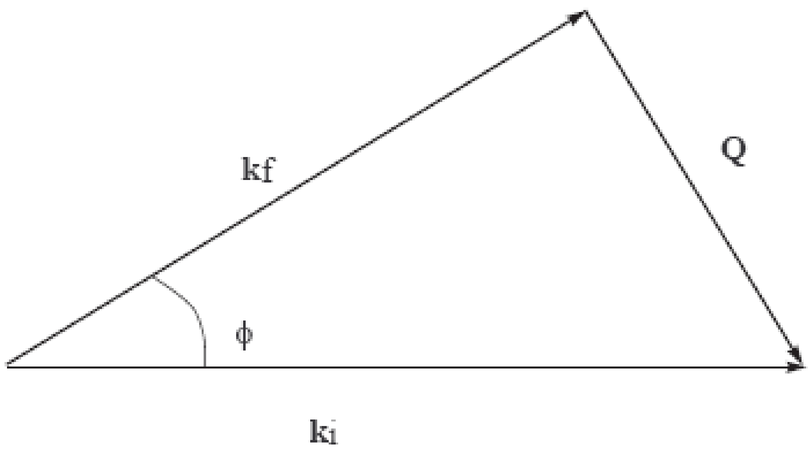

$$\hbar\omega = \frac{(\hbar\mathbf{k_i} - \hbar\mathbf{k_f})^{\mathbf{2}}}{2M} + \frac{(\hbar\mathbf{k_i} - \hbar\mathbf{k_f}) \cdot \hbar\mathbf{p}}{M}$$

$$\hbar\omega = \frac{\hbar^2\mathbf{Q^2}}{2M} + \frac{\hbar\mathbf{Q} \cdot \hbar\mathbf{p}}{M}$$

Measurements of momentum distributions using (deep) inelastic neutron scattering: two steps

$$Y_{jj'}(\mathbf{Q},t) = \langle e^{-i\mathbf{Q}\cdot\mathbf{R}_j}\; e^{i\mathbf{Q}\cdot\mathbf{R}_{j'}(t)}\rangle$$

1) Wave vector transfers in excess of 20 $Å^{-1}$: incoherent approximation → *j=j'*
2) Energy transfers in excess of 1 eV: short-time behaviour of the correlation function

Impulse approximation (IA): at the basis of
Deep Inelastic Neutron Scattering

Short-time behaviour

$$Y_{jj'}(\mathbf{Q},t) = \langle e^{-i\mathbf{Q}\cdot\mathbf{R}_j} \, e^{i\mathbf{Q}\cdot\mathbf{R}_{j'}(t)} \rangle$$

The operator $e^{-i\mathbf{Q}\cdot\mathbf{R}}$ couples the plane wave of the neutron with the position of the nucleus in the target system. The generic atom j has a position represented by the quantum mechanical operator $\mathbf{R}_j$. When the incident neutron energy is well in excess of the maximum energy available within the response spectrum of the target, the correlation function is approximated by its behavior at short times. The approximation involves a short time ($t \longrightarrow 0$) expansion of the atomic position operator :

$$\mathbf{R}_{j'}(t) = \mathbf{R}_{j'} + \frac{t}{M_{j'}}\mathbf{P}_{j'} \qquad (12)$$

where $\mathbf{P}$ is the momentum of the struck nucleus of mass M.

Short-time behaviour

$$\mathbf{R}_{j'}(t) = \mathbf{R}_{j'} + \frac{t}{M_{j'}}\mathbf{P}_{j'} \tag{12}$$

$$Y_{jj'}(\mathbf{Q},t) = \langle e^{-i\mathbf{Q}\cdot\mathbf{R}_j}\, e^{\left(i\mathbf{Q}\cdot\mathbf{R}_{j'} + \frac{it}{M_{j'}}\mathbf{Q}\cdot\mathbf{P}_{j'}\right)} \rangle \tag{13}$$

Remember that

$$[R_{\alpha j'}, P_{\beta j}] = i\hbar\, \delta_{jj'}\delta_{\alpha\beta} \tag{14}$$

and making use of the operator identity:

$$e^{A+B} = e^A e^B e^{1/2[A,B]}, \tag{15}$$

which holds when $[A, B]$ commutes with both A and B, then the exponentials in eq. 13 can be written

$$e^{-i\mathbf{Q}\cdot\mathbf{R}_j}\, e^{\left(i\mathbf{Q}\cdot\mathbf{R}_{j'} + \frac{it}{M_{j'}}\mathbf{Q}\cdot\mathbf{P}_{j'}\right)} = \tag{16}$$

$$= e^{-i\mathbf{Q}\cdot\mathbf{R}_j + i\mathbf{Q}\cdot\mathbf{R}_{j'} + \frac{it}{M_{j'}}\mathbf{Q}\cdot\mathbf{P}_{j'} + 1/2[\mathbf{Q}\cdot\mathbf{R}_j, (\mathbf{Q}\cdot\mathbf{R}_{j'} + \frac{t}{M_{j'}}\mathbf{Q}\cdot\mathbf{P}_{j'})]} \tag{17}$$

The commutator in the above equation involves position operators at the same time (=0), and commutation following eq.12.

Short-time behaviour

The result is:

$$Y_{jj'}(\mathbf{Q},t) = e^{\frac{i\hbar t Q^2}{2M_j}\delta_{jj'}} \langle e^{i\mathbf{Q}(\mathbf{R}_{j'}-\mathbf{R}_j)+\frac{it}{M_{j'}}\mathbf{Q}\cdot\mathbf{P}_{j'}} \rangle \qquad (18)$$

Large Q behavior: considering that the spatial scale of the scattering event is given by 1/Q, we can assume that correlations between the positions of different nuclei are absent and the incoherent approximation holds. The exponentials containing position operators of different nuclei in the above correlation function will oscillate rapidly from atom to atom and cancel out on average.

$$Y_j(\mathbf{Q},t) = e^{\frac{i\hbar t Q^2}{2M_j}} \langle e^{\frac{it}{M_j}\mathbf{Q}\cdot\mathbf{P}_j} \rangle \qquad (19)$$

Short-time behaviour: Dynamical structure factor

$$S(\mathbf{Q},\omega) = \frac{1}{N\ 8\pi^2\hbar} \sum_j \int_{-\infty}^{\infty} dt\ e^{\left(-i\omega t + \frac{i\hbar t Q^2}{2M_j}\right)} \langle e^{\frac{it}{M_j}\mathbf{Q}\cdot\mathbf{P}_j} \rangle \tag{20}$$

$$\left\langle e^{\frac{i\,t}{M_j}\vec{Q}\cdot\vec{P}_J} \right\rangle = \int d\vec{p}\ n(\vec{p})\, e^{\frac{i\,t}{M_j}\vec{Q}\cdot\vec{p}}$$

That is, the average is taken over the distribution of individual momenta **Pj**, that is $n(\vec{p})$

Short-time behaviour: Dynamical structure factor

After some calculations

$$S(\mathbf{Q},\omega)_{IA} = \frac{1}{4\pi\hbar}\int_{-\infty}^{\infty} d\mathbf{p}\, n(\mathbf{p})\, \delta(\omega - \frac{\hbar\, Q^2}{2M} - \frac{\hbar}{M}\mathbf{Q}\cdot\mathbf{p})$$

For a single target atom of mass M at rest, the scattering will be centred at

$$\delta(\omega - \frac{\hbar\, Q^2}{2M})$$

That is , S(Q,ω) will be peaked at

$$\hbar\omega_R = \frac{\hbar^2 Q^2}{2M}$$

NOT ALL THE TARGET ATOMS WILL BE AT REST, AND A PROBABILITY DISTRIBUTION FUNCTION (PDF) OF ATOMIC MOMENTUM WILL WEIGHT THE PEAK OF S(Q, ω) TO ACCOUNT FOR THE SPREAD OF ATOMIC MOMENTA

Energy and wave vector transfer are coupled in DINS!

Now, since ω and $\mathbf{Q}$ are closely related in the IA scattering regime it is useful to introduce a new variable y which couples wavevector and energy transfer (G. B.West, *Phys. Rep.*, **18**, 263 (1975).):

$$y = \frac{M}{\hbar^2\, Q}(\hbar\omega - \hbar\omega_R) \qquad (36)$$

and, considering that

$$\hbar\omega = \frac{\hbar^2(\mathbf{p}+\mathbf{Q})^2}{2M} - \frac{\hbar^2\,\mathbf{p}^2}{2M} \qquad (37)$$

, then y just represents the component of atomic wavevector along the scattering direction (i.e. $y = \mathbf{p}\cdot\widehat{\mathbf{Q}}$).

Units : inverse Angstroms!

Energy and wave vector transfer are coupled in DINS!

Rearranging in terms of the new variable

$$S(\mathbf{Q},\omega)_{IA} = \frac{M}{4\pi\hbar^2\, Q}\int_{-\infty}^{\infty} dp_x dp_y\; n(p_x, p_y, y)$$

Introduce a new function: the "Neutron Compton Profile" (NCP)

$$J(y) = \frac{2\pi\hbar^2 Q}{M} S(\mathbf{Q},\omega)_{IA}$$

For isotropic systems $$J(y) = \int_{|y|}^{\infty} dp\; p\; n(p)$$

J(y) symmetric and maximum for y=0

DESIGNING AND BUILDING A DINS SPECTROMETER: Deep Inelastic Neutron Scattering Timeline

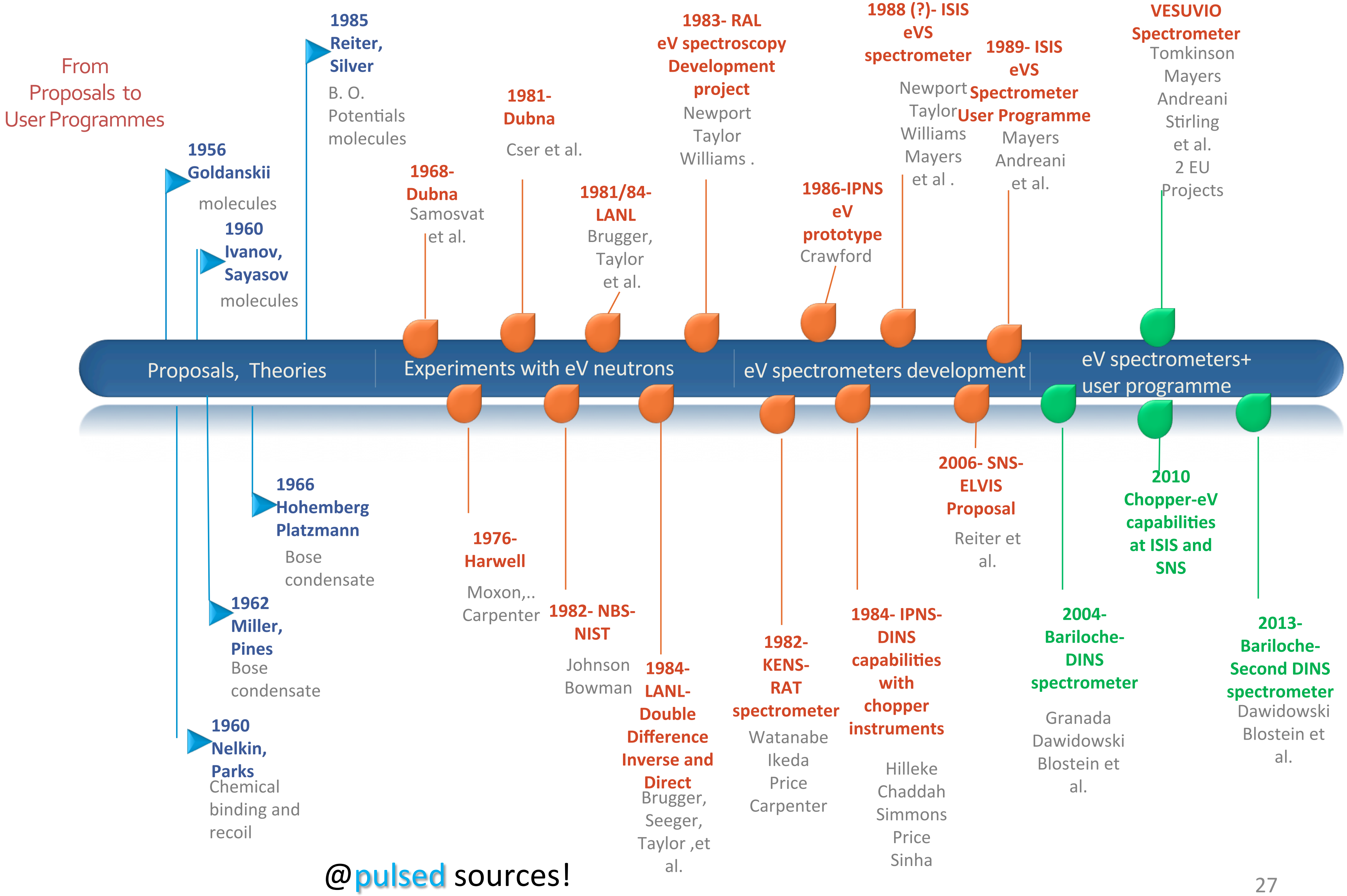

DESIGNING AND BUILDING A DINS NEUTRON INSTRUMENT: LAYOUT AND DINS SPECIFIC CONFIGURATIONS . 1) GEOMETRY

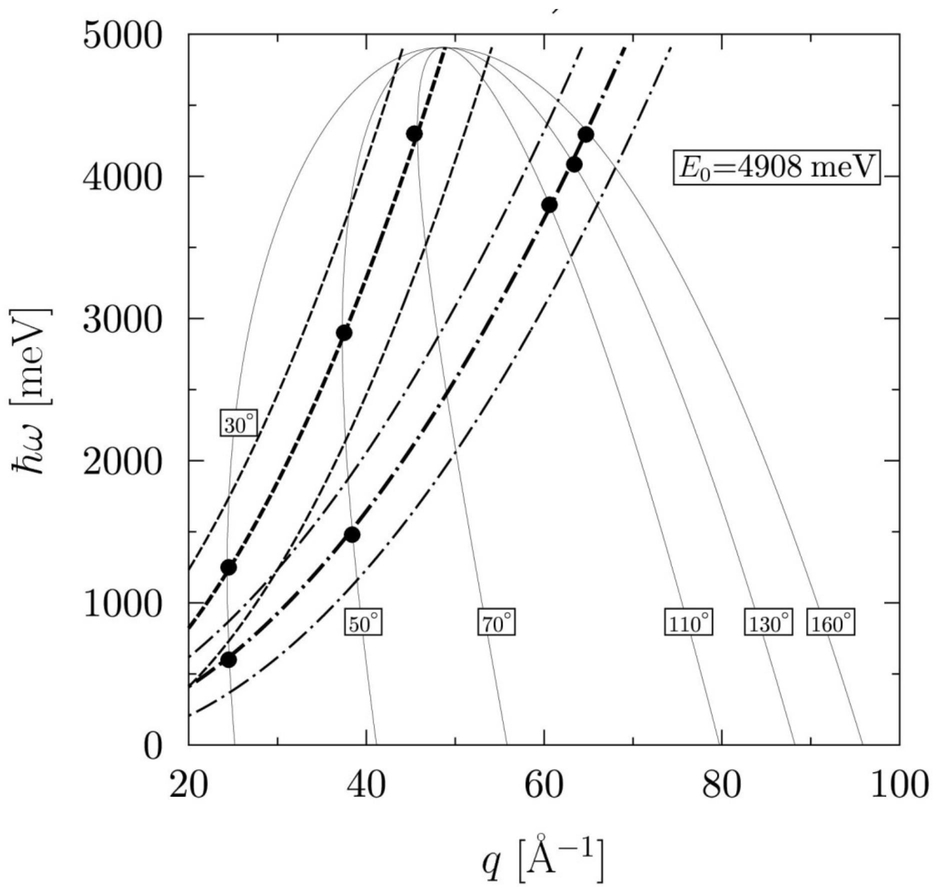

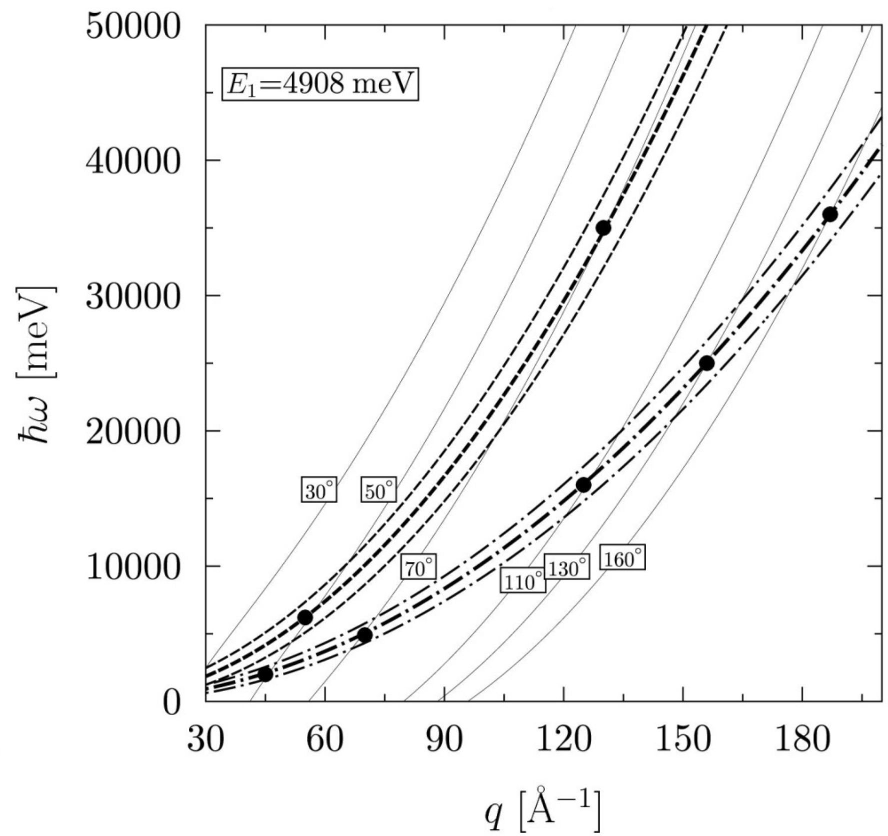

In principle both direct and inverse geometries can be used Brugger, Taylor, Soper et al. (1984)

DESIGNING AND BUILDING A DINS NEUTRON INSTRUMENT: LAYOUT AND DINS SPECIFIC CONFIGURATIONS . 1) GEOMETRY

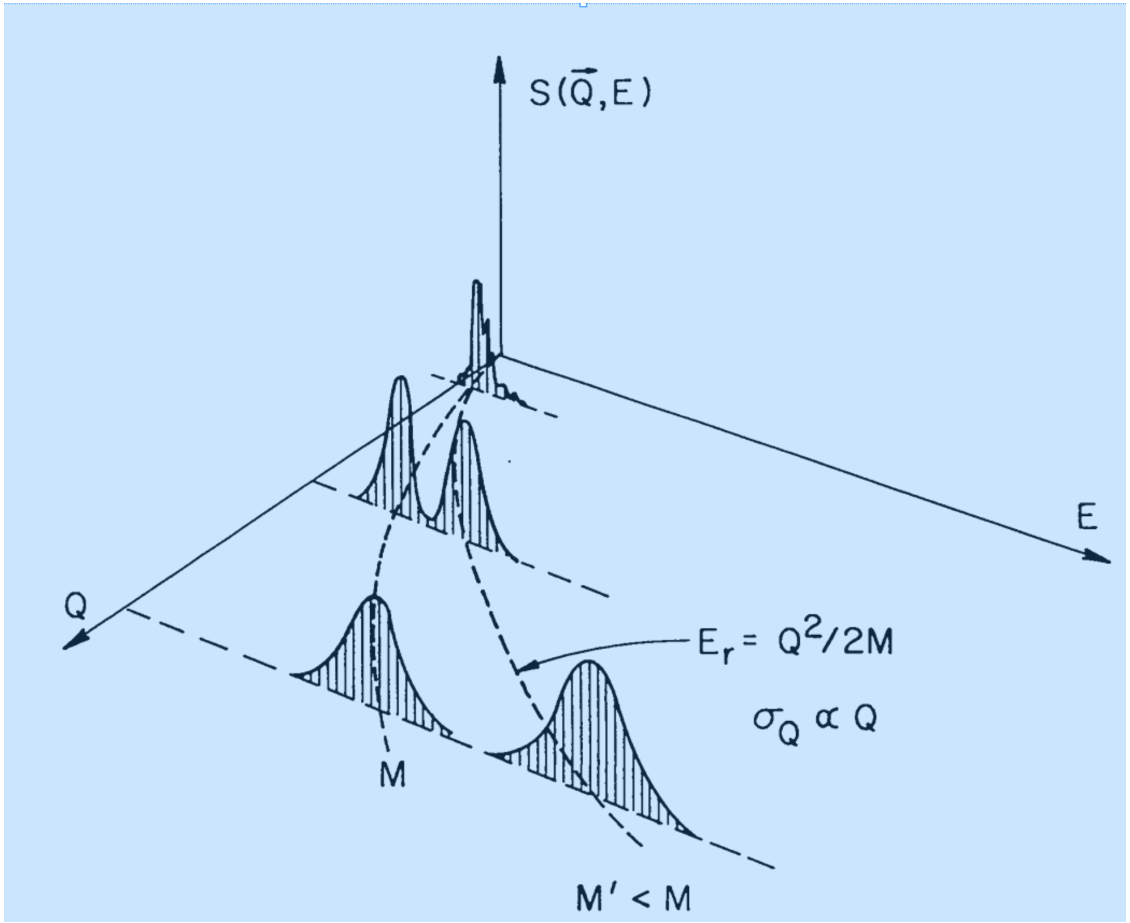

From R.O. Simmons LA-10227-C (1984)

In principle both direct and inverse geometries can be used Brugger, Taylor, Soper et al. (1984)

For hydrogen containing samples, data for direct geometry can be analysed only in constant-q mode. Limited q-ω range

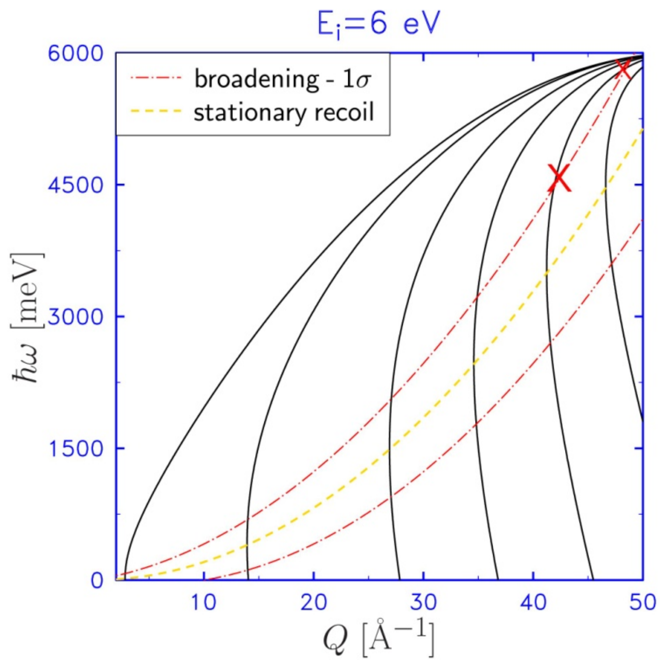

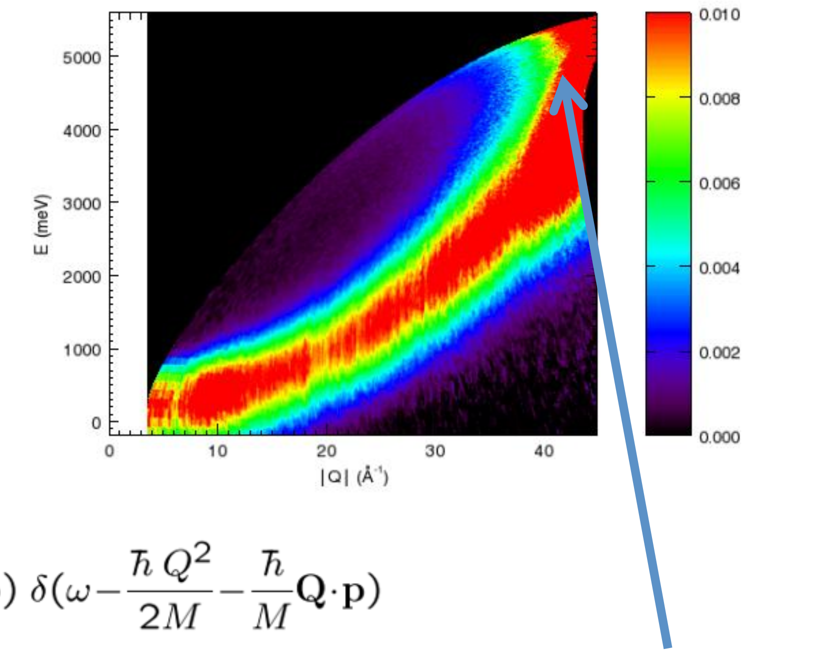

$$n(\mathbf{p})\ \delta(\omega - \frac{\hbar\, Q^2}{2M} - \frac{\hbar}{M}\mathbf{Q}\cdot\mathbf{p})$$

Extra intensity !

1- Stationary proton recoil is broadened by the proton momentum distribution -std dev approx 5 Å^{-1}

Good measurements need to scan broadenings at +/- 25 Å^{-1}

2- X mark the loci where the same broadening (proton's momentum) appears at two different couple of values of energy and wave vectors at the SAME SCATTERING ANGLE !

Hydrogen recoil measurements on SEQUOIA at the SNS

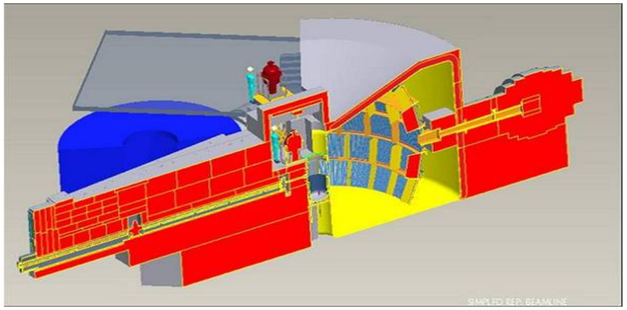

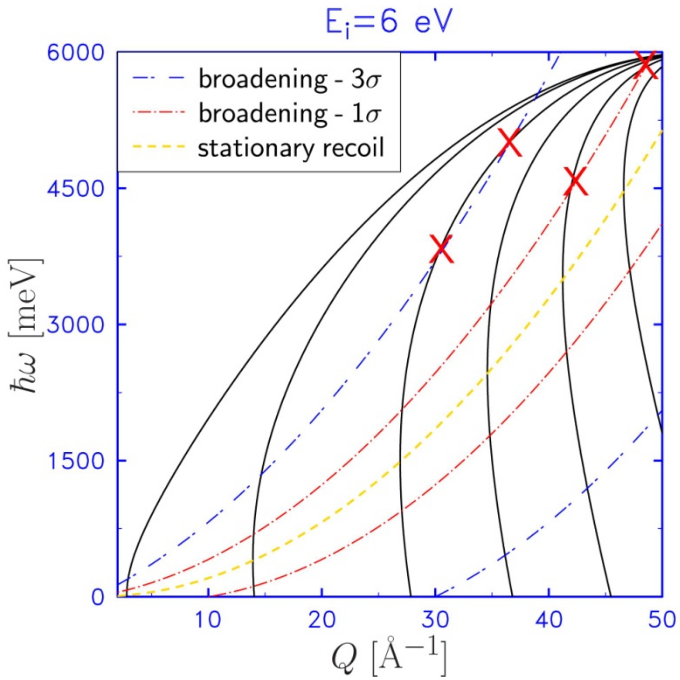

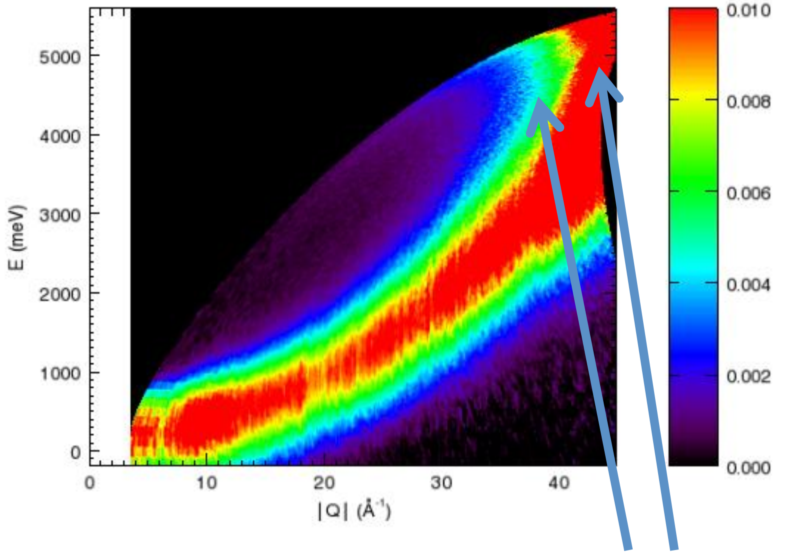

Extra intensity !

3- constant angle≠ constant-Q AND constant angle*Jacobian≠ constant-Q

4- constant-Q strips rebinning is OK

Historical Weather For 2010 in Oak Ridge, Tennessee, USA

Location

This report describes the historical weather record at the Oak Ridge (Oak Ridge, Tennessee, United States) during 2010. This station has records back to January 1999.

Oak Ridge, Tennessee has a warm humid temperate climate with hot summers and no dry season. The area within 40 km of this station is covered by *forests* (86%), *lakes and rivers* (6%), *built-up areas* (5%), and *croplands* (4%)

Nearby Stations

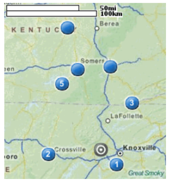

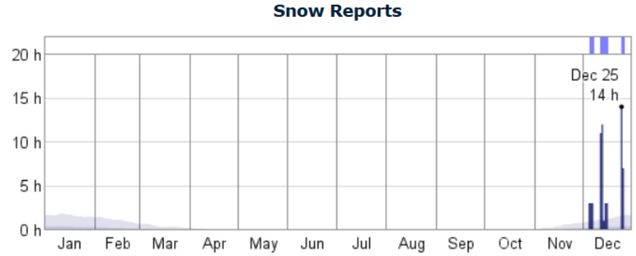

DESIGNING AND BUILDING A DINS NEUTRON INSTRUMENT: LAYOUT AND DINS SPECIFIC CONFIGURATIONS . 1) Best GEOMETRY is INVERSE

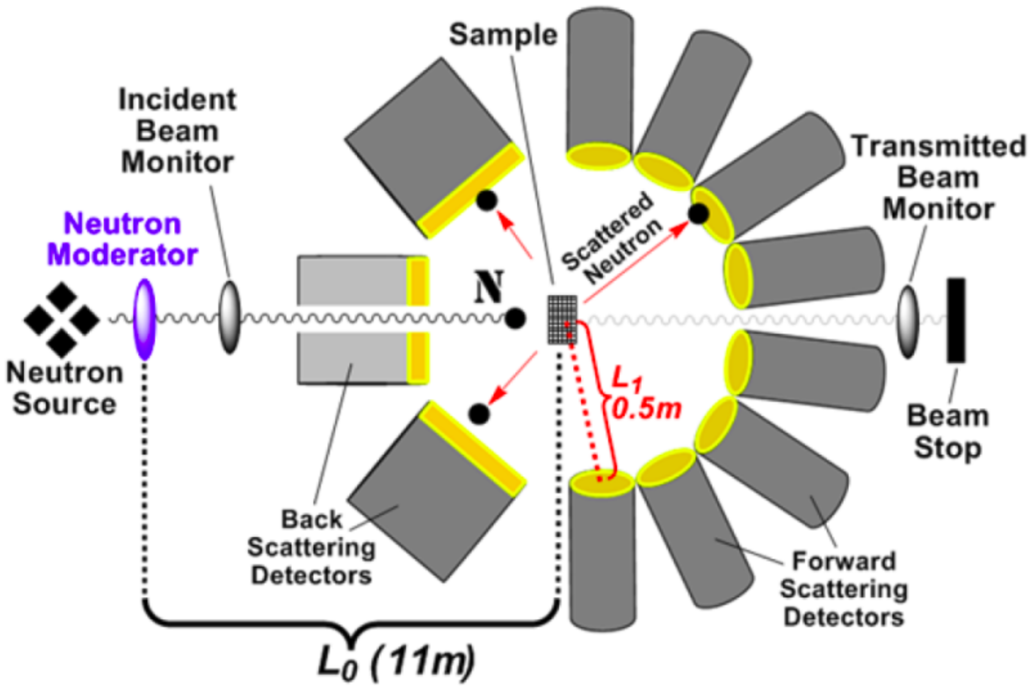

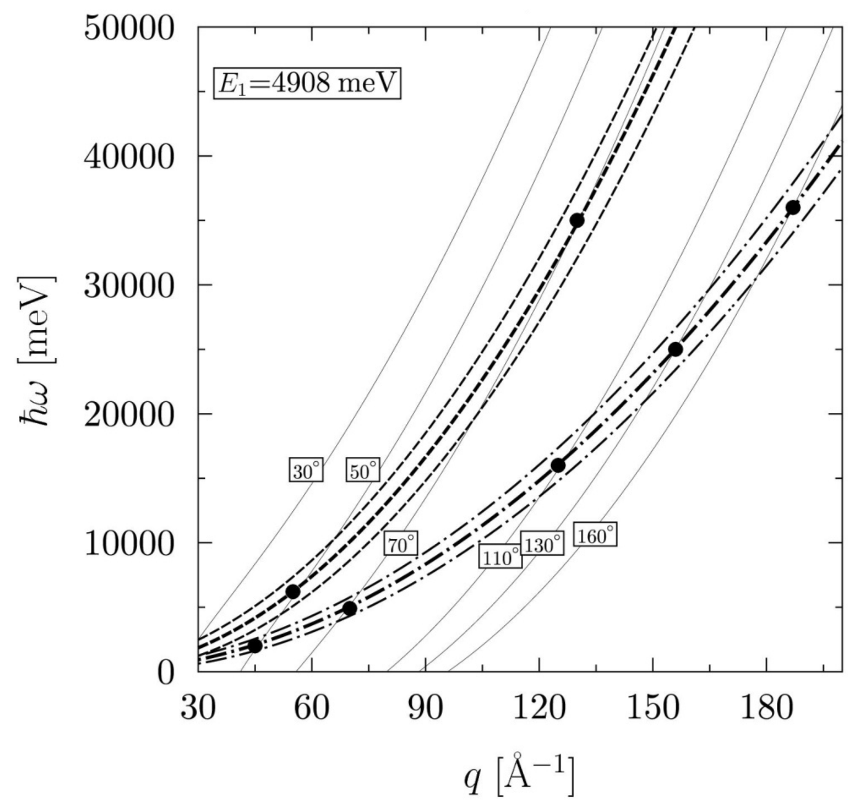

L_0 is long, L_1 is short

DESIGNING AND BUILDING A DINS NEUTRON INSTRUMENT: LAYOUT AND DINS SPECIFIC CONFIGURATIONS . 2) Resonant energy analysers

Crystal monochromators are inefficient above 1 eV; Choppers in inverse geometry are impractical; Neutron absorption resonances are used

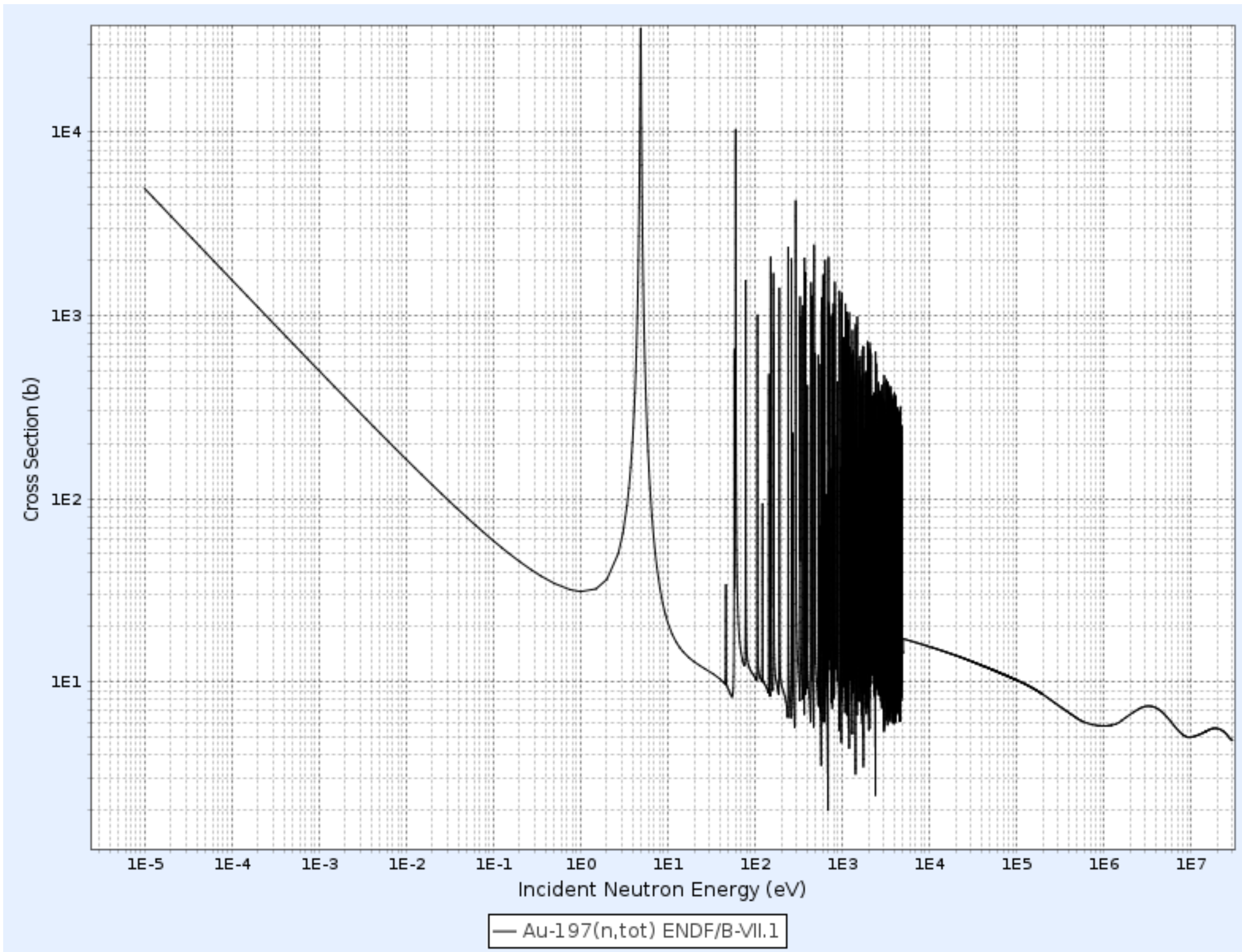

DESIGNING AND BUILDING A DINS NEUTRON INSTRUMENT: LAYOUT AND DINS SPECIFIC CONFIGURATIONS . 2) Resonant energy analysers

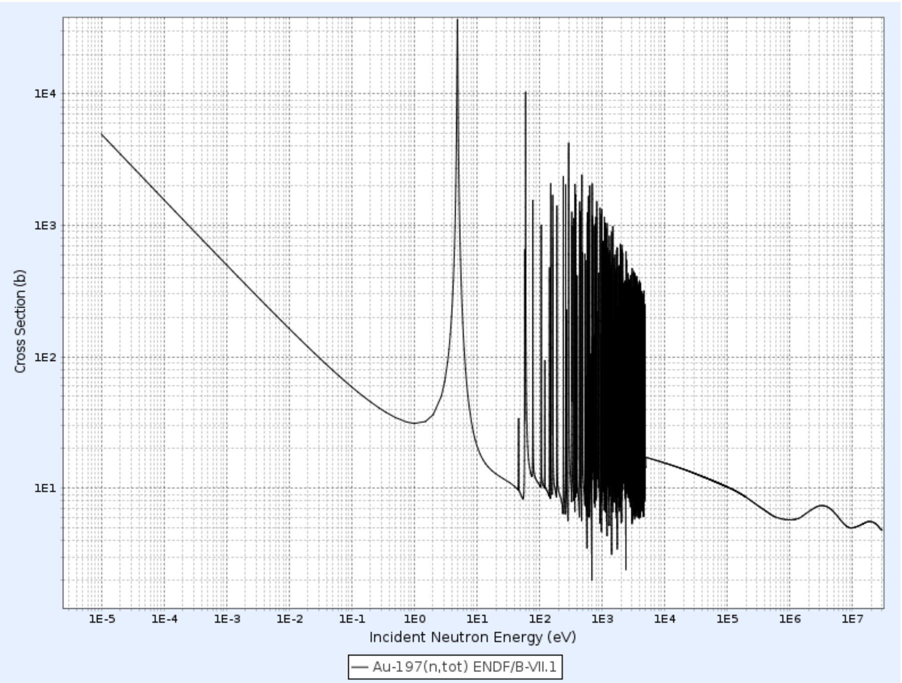

Metallic foils showing resonances are a sort of "passive" energy analysers

Following resonant absorption:

1) **Neutrons with energies equal or near the resonance are removed from the scattered beam**
2) **A prompt (instantaneous) gamma emission is produced**

DESIGNING AND BUILDING A DINS NEUTRON INSTRUMENT: LAYOUT AND DINS SPECIFIC CONFIGURATIONS . 2) Resonant energy analysers

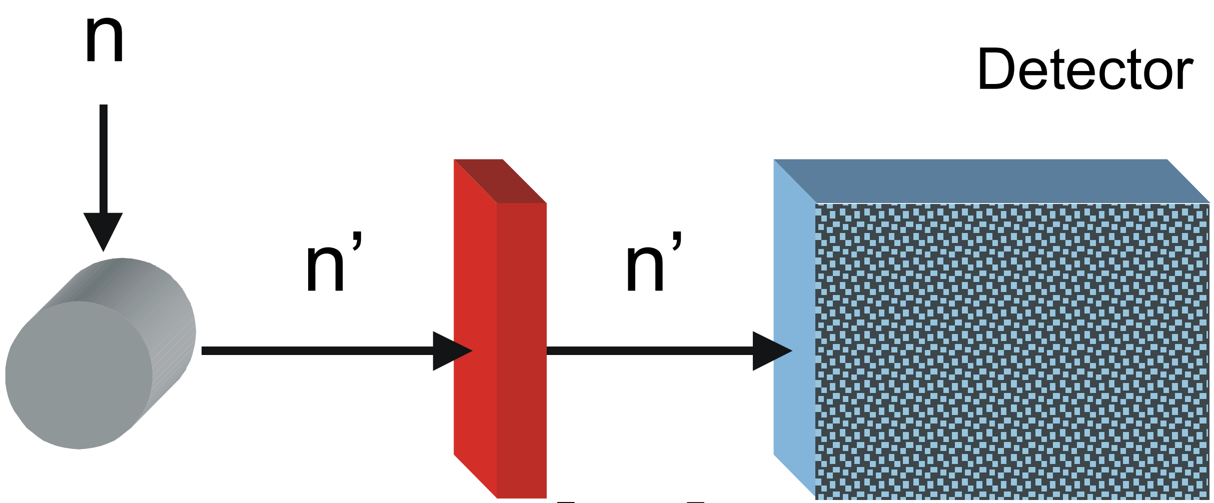

Fixed v_1 (final v)
(Inverse Geometry)

$$t = \frac{L_0}{v_0} + \frac{L_1}{v_1} \rightarrow v_0$$

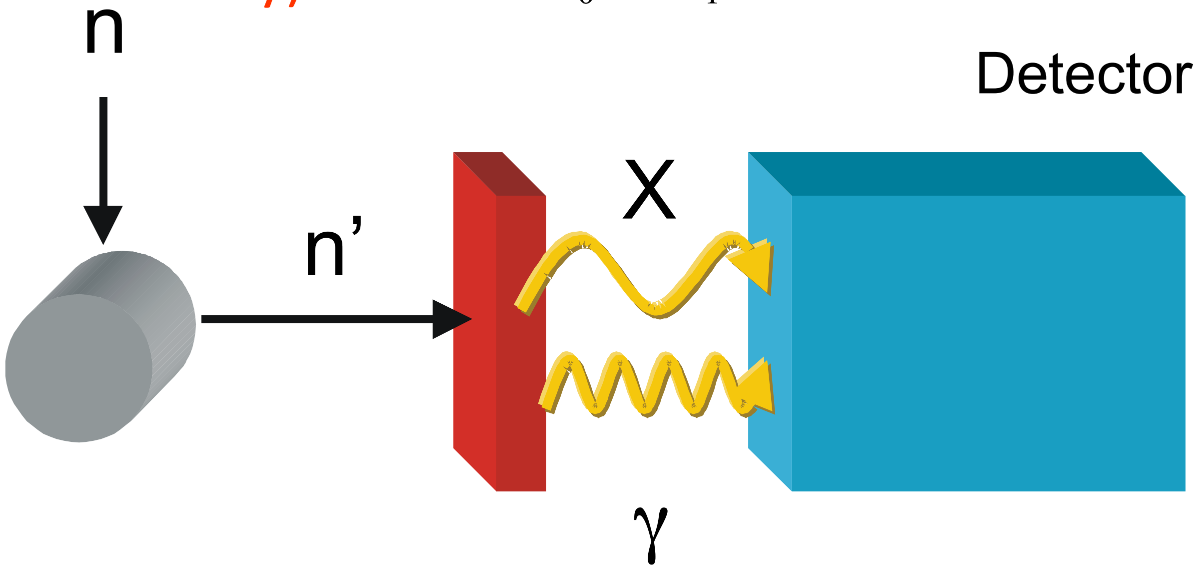

DESIGNING AND BUILDING A DINS NEUTRON INSTRUMENT: LAYOUT AND DINS SPECIFIC CONFIGURATIONS . 2) Resonant energy analysers

1) Neutrons with energies equal or near the resonance are removed from the scattered beam

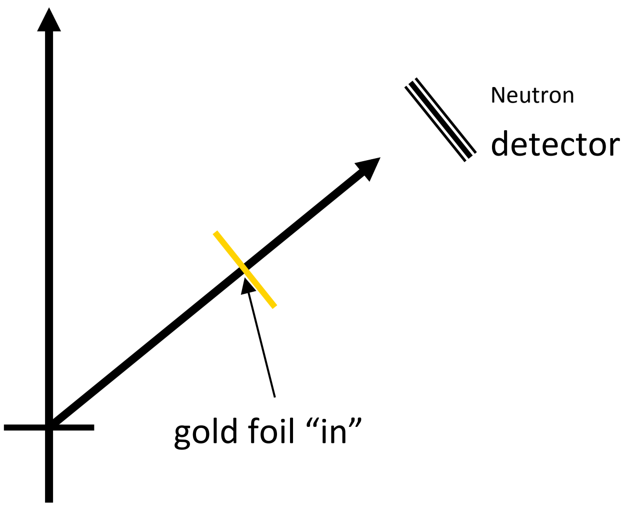

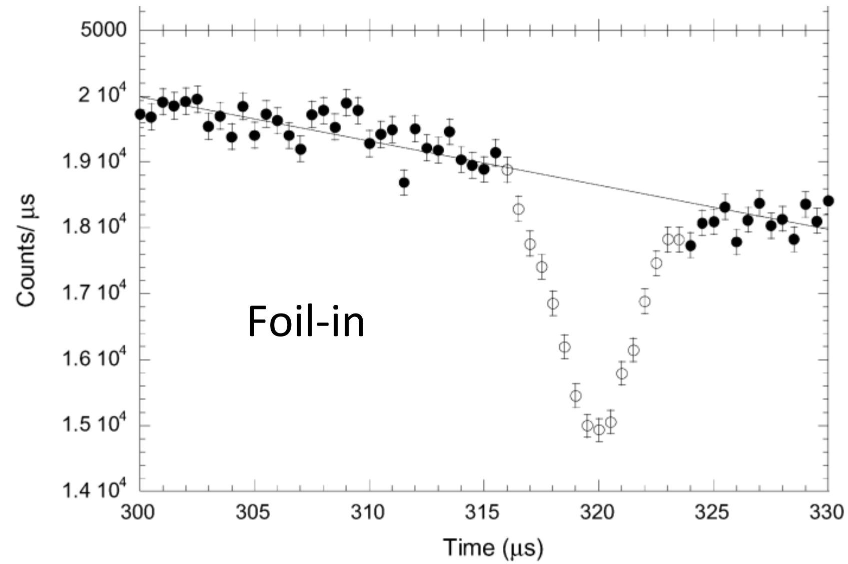

NEEDS MOVING COMPONENTS:
Resonant foils cycled in and out of the scattered beam

Cts = Foil out – foil in

DESIGNING AND BUILDING A DINS NEUTRON INSTRUMENT: LAYOUT AND DINS SPECIFIC CONFIGURATIONS . 2) Resonant energy analysers

2) The prompt (instantaneous) gamma emission is recorded

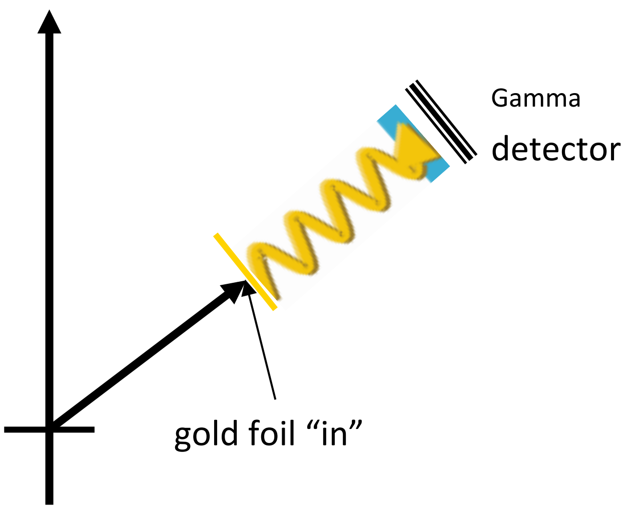

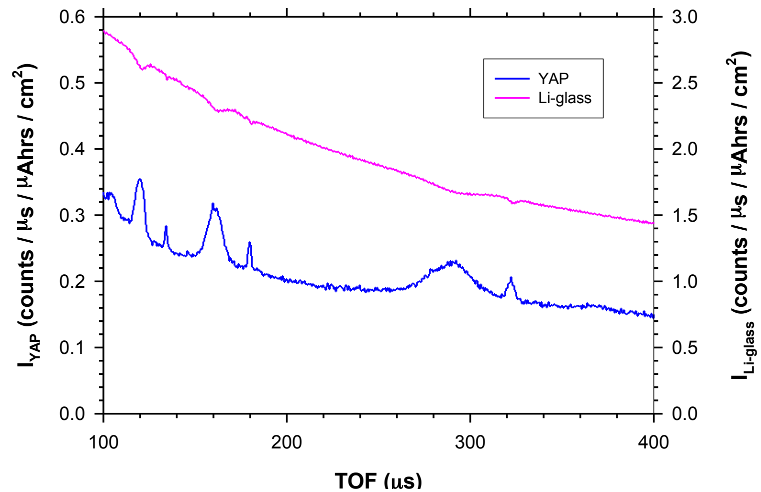

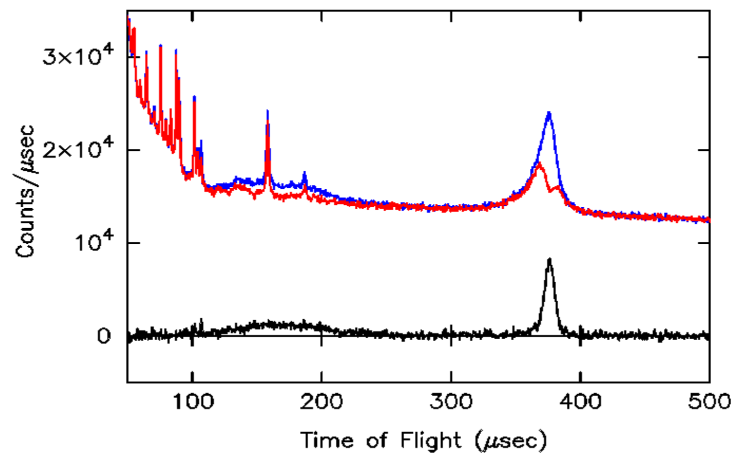

In principle no NEED of MOVING COMPONENTS: In practice resonant foils are cycled in and out to improve Signal to Background

DESIGNING AND BUILDING A DINS NEUTRON INSTRUMENT: LAYOUT AND DINS SPECIFIC CONFIGURATIONS . 2) Resonant energy analysers

Total energy transfer resolution

Table 3

Resonance energy E_1 and FWHM, ΔE_1 for the different foils at room temperature, taken as FWHM from the experimental neutron scattering cross section data available at [61]. ΔE_1 represents the energy contribution to the instrument resolution. In the case of ^{238}U the value at a temperature $T = 77$ K is also reported, indicated with a (*). The columns 4–8 report the calculated resolution $\Delta\hbar\omega$ for selected values of the energy transfer $\hbar\omega$.

Filter	E_1 (eV)	ΔE_1 (meV)	$\Delta\hbar\omega$ (meV)				
			$\hbar\omega = 10$ meV	$\hbar\omega = 500$ meV	$\hbar\omega = 3$ eV	$\hbar\omega = 7$ eV	$\hbar\omega = 20$ eV
^{149}Sm	0.872	83	98	113	224	492	1848
^{240}Pu	1.06	56	66	74	133	272	965
^{185}Re	2.16	58	69	73	99	157	429
^{242}Pu	2.67	71	85	89	114	167	416
^{197}Au	4.91	182	216	221	252	313	581
^{238}U	6.67	103 (66*)	125	128	144	174	307
^{187}Os	12.7	100	135	138	151	177	286
^{150}Sm	20.7	261	331	334	351	379	495
^{238}U	20.9	177	243	246	262	290	404
^{238}U	36.6	242	387	391	411	446	578
^{238}U	66.0	320	701	707	736	784	952
^{139}La	72.1	436	844	850	879	928	1098
^{168}Er	79.7	120	785	791	826	883	1075
^{238}U	102.6	410	1210	1217	1254	1315	1521

$$2\% \leq \Delta\hbar\omega/\hbar\omega \leq 4\%$$

DESIGNING AND BUILDING A DINS NEUTRON INSTRUMENT: LAYOUT AND DINS SPECIFIC CONFIGURATIONS . 2) Resonant energy analysers

Momentum resolution- similar to X-Ray Compton scattering

Electrons, using ID16 at ESRF

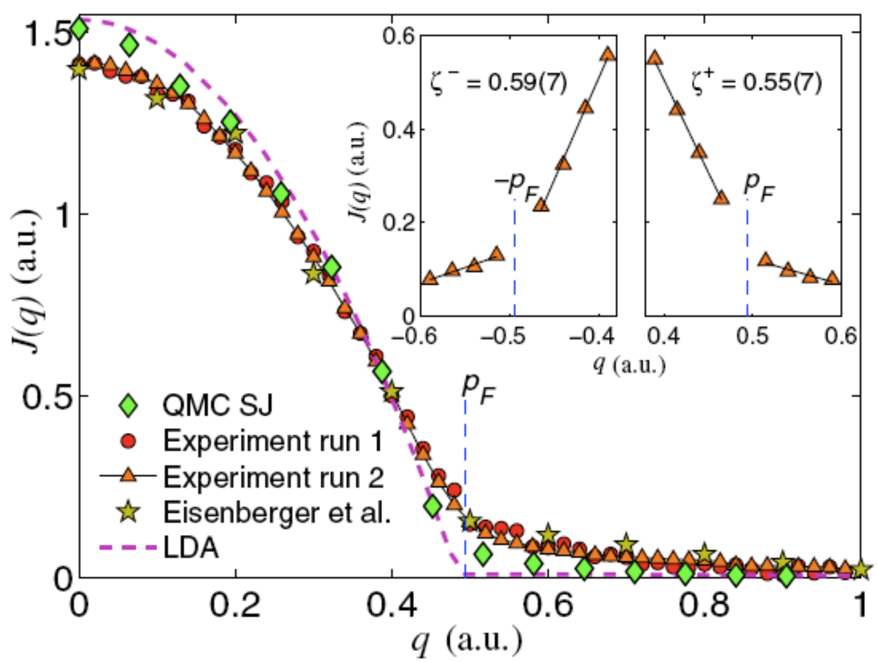

Compton profile of Na; p- resolution≈13%
S. Huotari et al, PRL 105, 086403 (2010)

Protons, using VESUVIO at ISIS

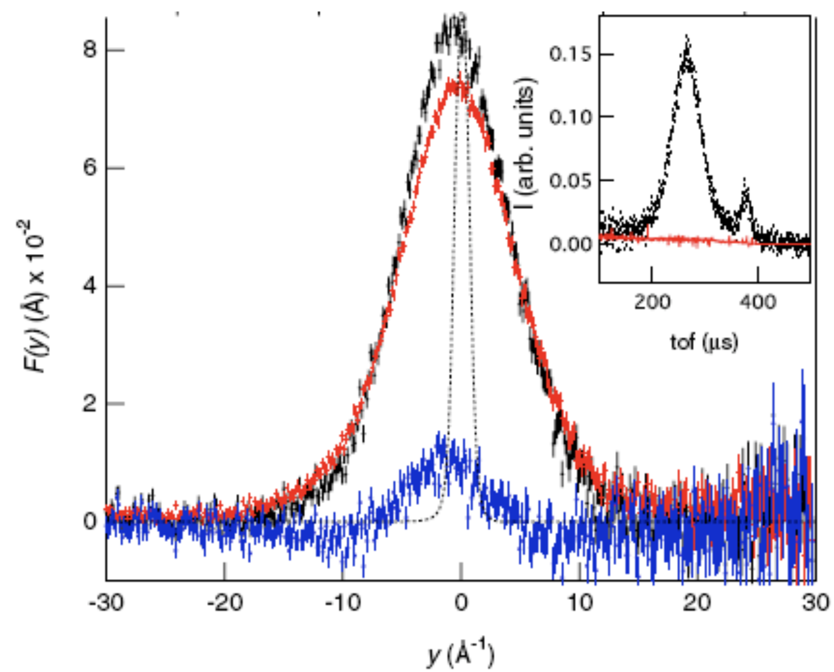

Neutron Compton profile of water; p-resolution≈14%
A. Pietropaolo et al, PRL 100, 127802 (2008)

$$q = \vec{p} \cdot \hat{q}$$

$$y = \frac{\vec{p}}{\hbar} \cdot \hat{q}$$

DESIGNING AND BUILDING A DINS NEUTRON INSTRUMENT: LAYOUT AND DINS SPECIFIC CONFIGURATIONS . 3) Detectors for multi-eV neutrons

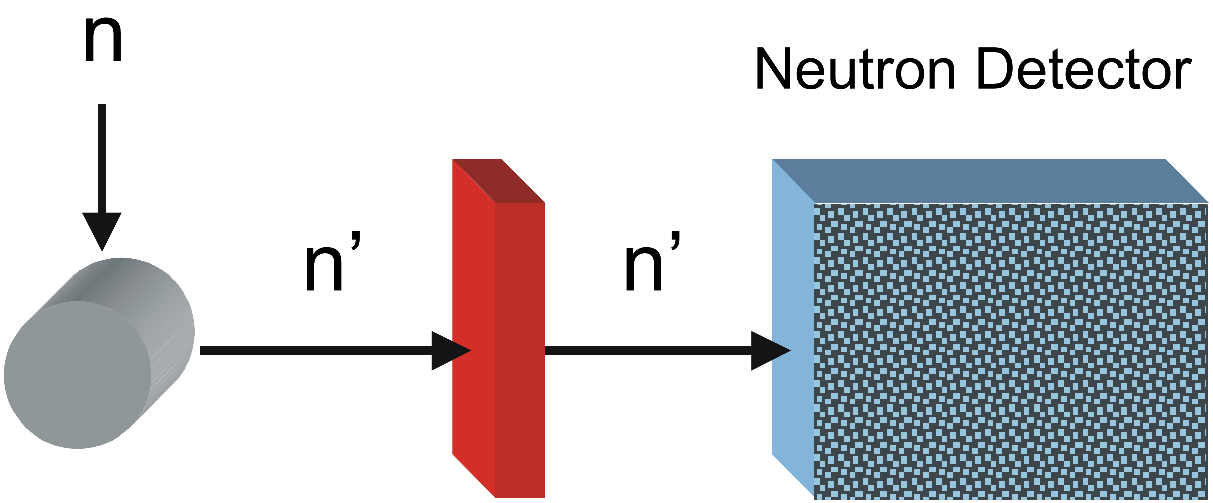

GS20 ^{6}Li glass scintillator

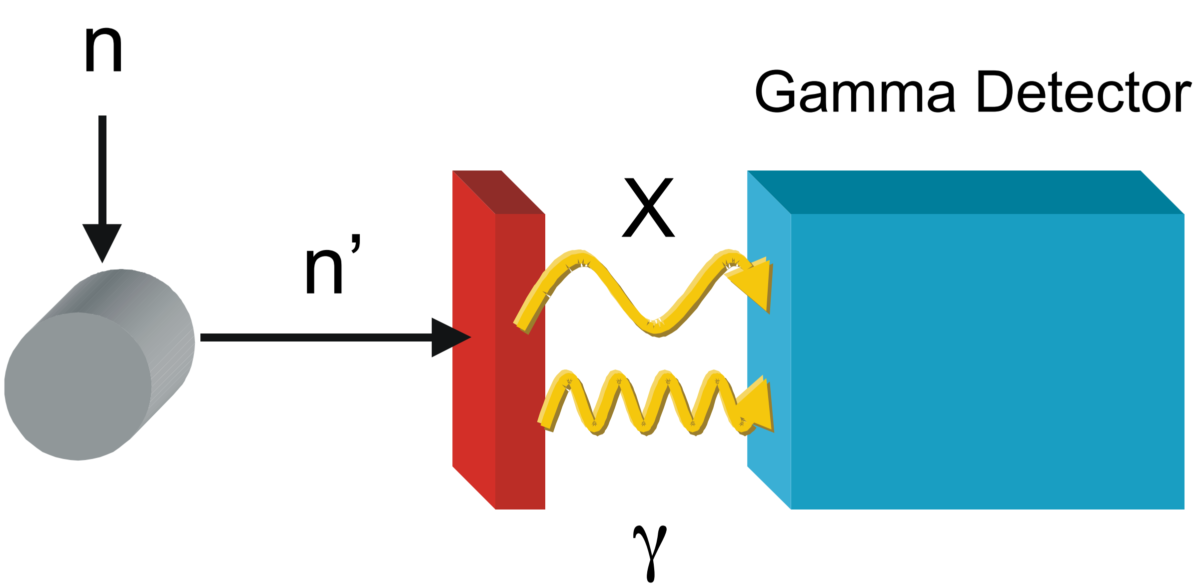

YAP gamma scintillator
Negligible neutron sensitivity

DESIGNING AND BUILDING A DINS NEUTRON INSTRUMENT: LAYOUT AND DINS SPECIFIC CONFIGURATIONS . 3) Detectors for multi-eV neutrons

Comparative measurements have shown that YAP gamma scintillators have better performance

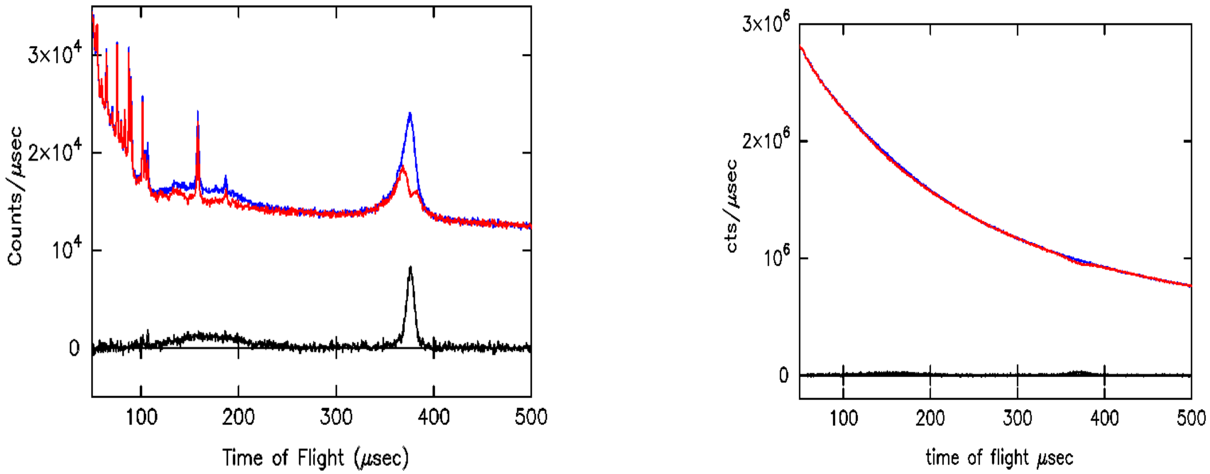

	H		Zr	
	peak	error	peak	error
YAP	$5\ 10^{-2}$	$2\ 10^{-3}$	$3\ 10^{-2}$	$2\ 10^{-3}$
Li-glass	$5\ 10^{-2}$	$3\ 10^{-3}$	$3\ 10^{-2}$	$3\ 10^{-3}$

DESIGNING AND BUILDING A DINS NEUTRON INSTRUMENT: LAYOUT AND DINS SPECIFIC CONFIGURATIONS . 3) Detectors for multi-eV neutrons

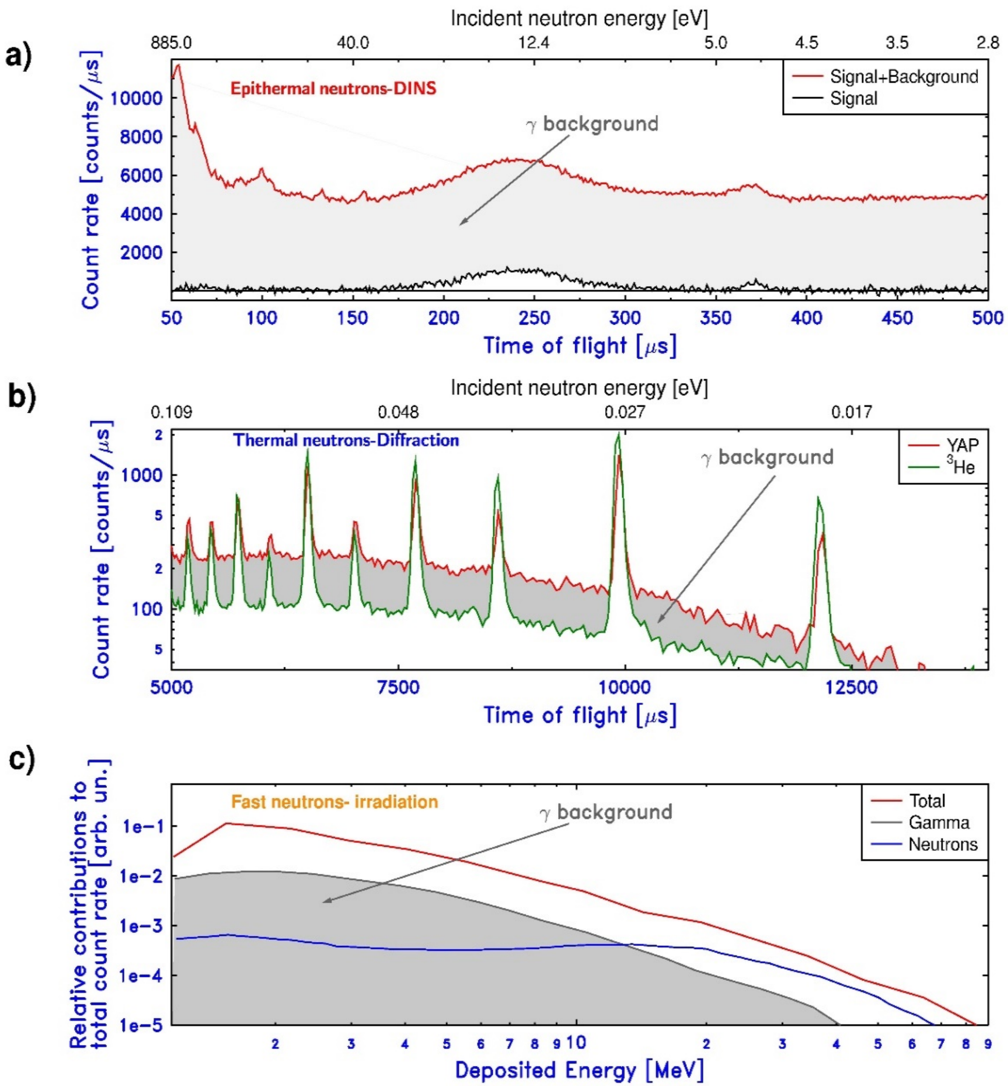

DINS signal/gamma background= 15%

Knowledge and characterisation of gamma background is necessary! Well, just like any other instrument…

DESIGNING AND BUILDING A DINS NEUTRON INSTRUMENT: LAYOUT AND DINS SPECIFIC CONFIGURATIONS . 3) Detectors for multi-eV neutrons

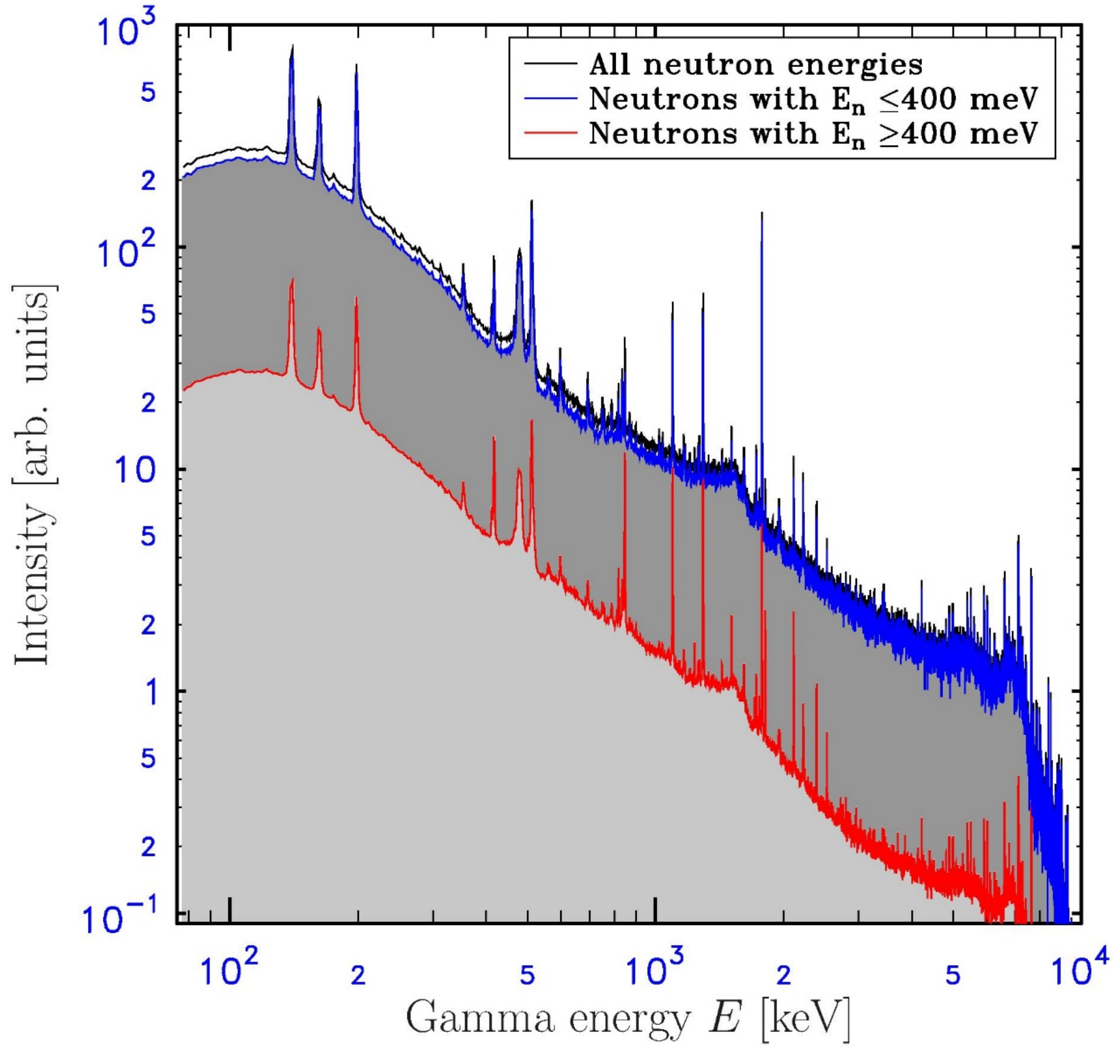

Knowledge and characterisation of gamma background is necessary! Well, just like any other instrument…

VESUVIO LAYOUT, ISIS TS-1

VESUVIO
within the
Molecular Spectroscopy Group
led by F.Fernandez-Alonso

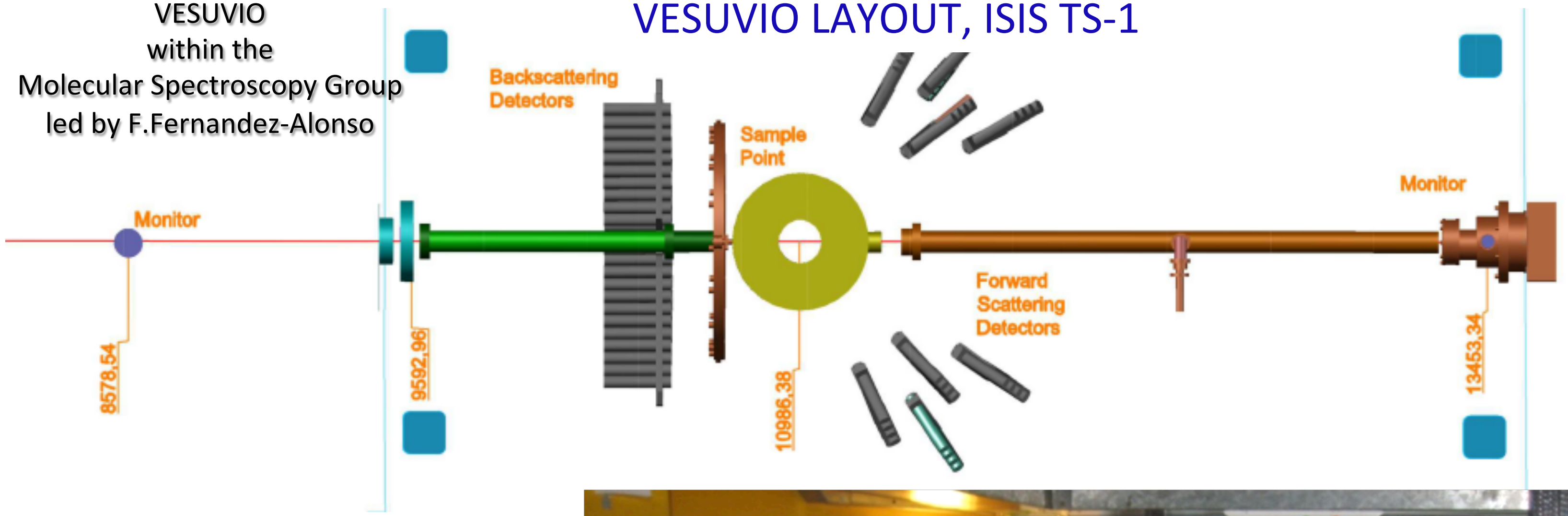

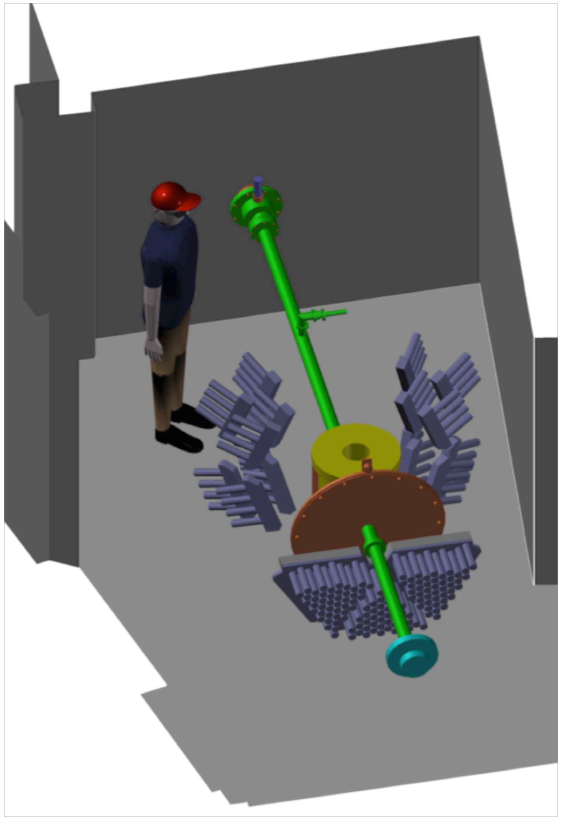

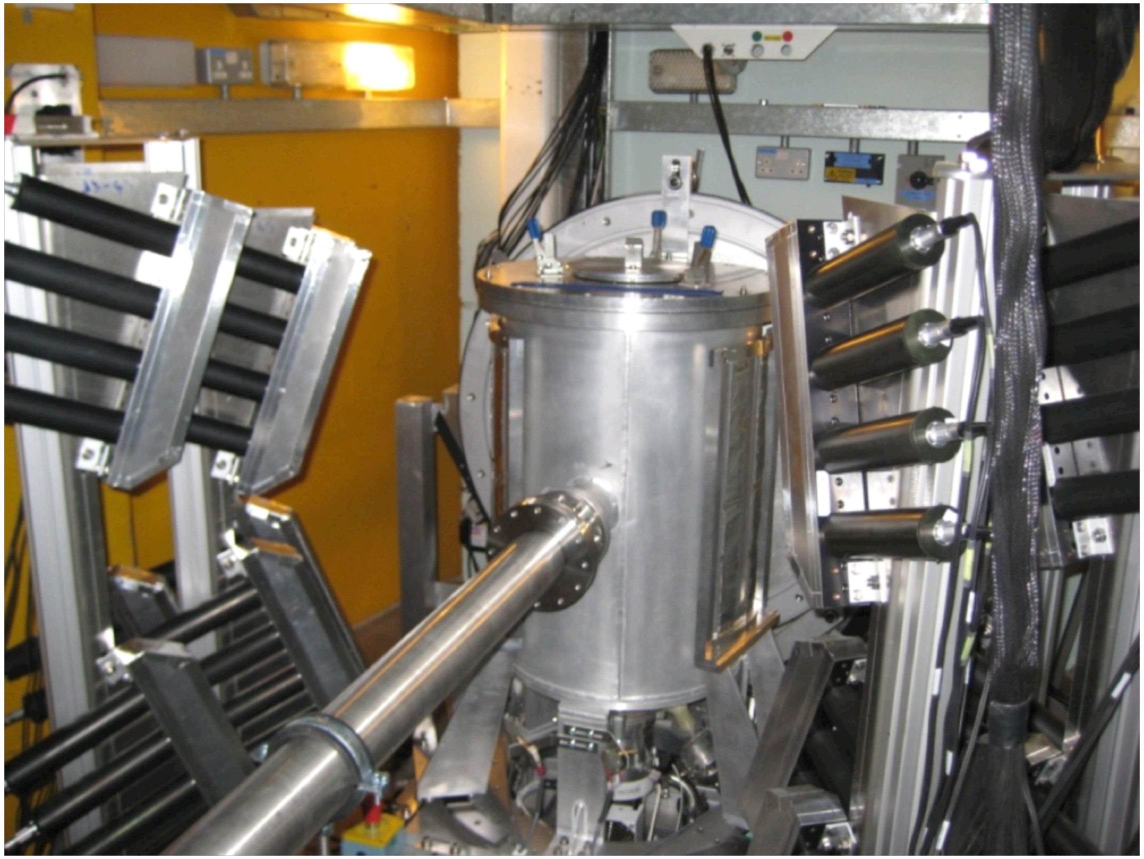

DINS SPECTROMETER in Bariloche - LAYOUT

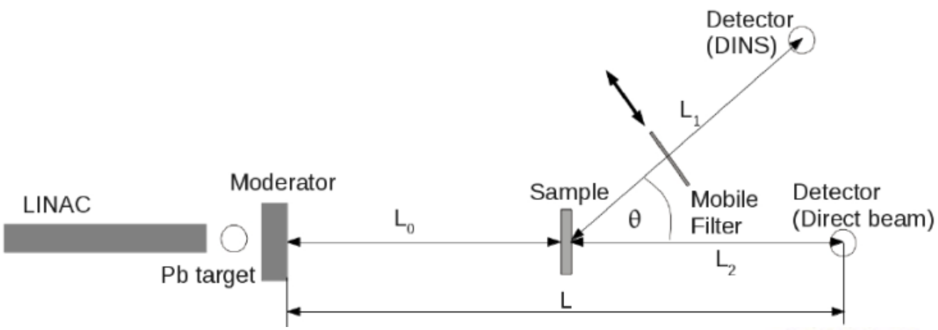

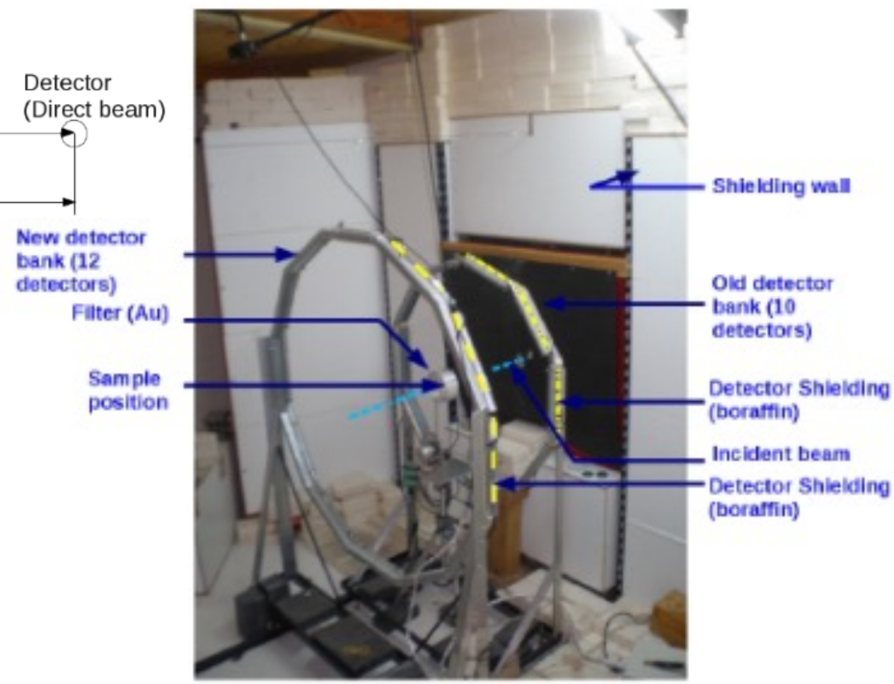

ISIS instruments set the trends for the use of eV neutron beams- examples

Direct Measurement of Competing Quantum Effects on the Kinetic Energy of Heavy Water upon Melting G. Romanelli et al., J. Phys. Chem. Lett. (2013)- **VESUVIO**

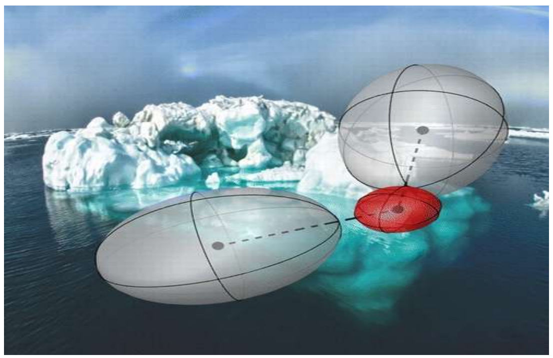

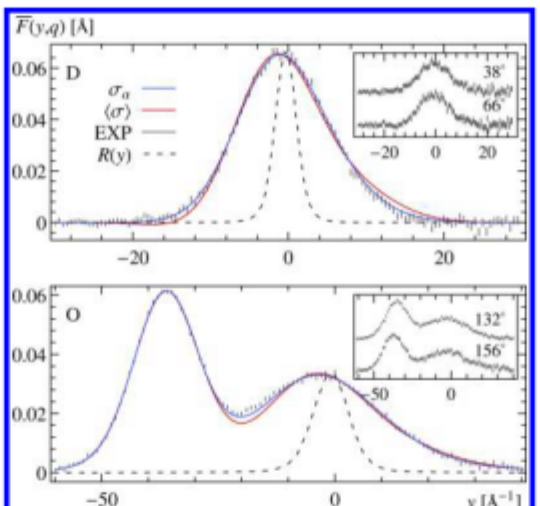

Deep Inelastic Neutron Scattering- a spectroscopic counterpart of total scattering. "Evolution of Hydrogen Dynamics in Amorphous Ice with Density", A. Parmentier et al., J. Phys. Chem. Lett. (2015)- **VESUVIO**

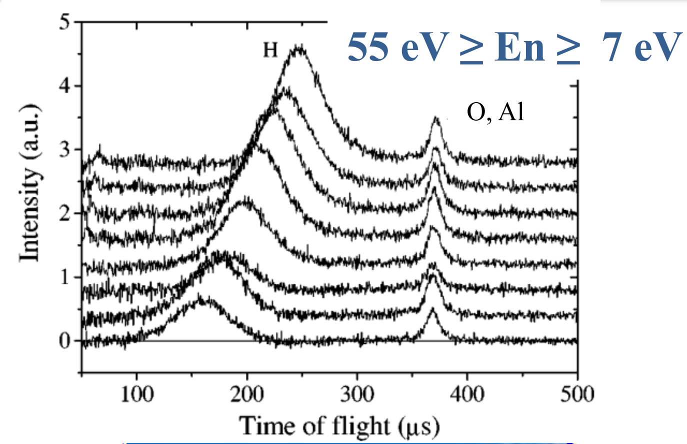

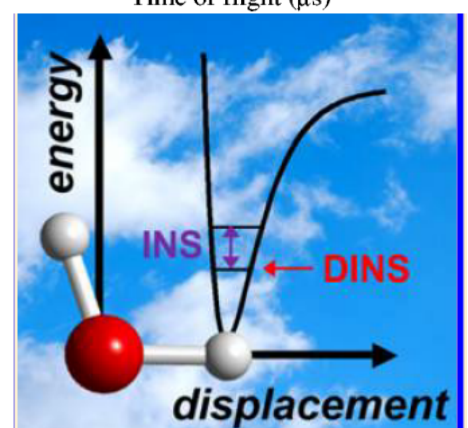

“Nuclear dynamics in the metastable phase of the solid acid caesium hydrogen sulfate”, M. Krzystyniak et al., PCCP (2015)- **VESUVIO.**

Energy-related materials

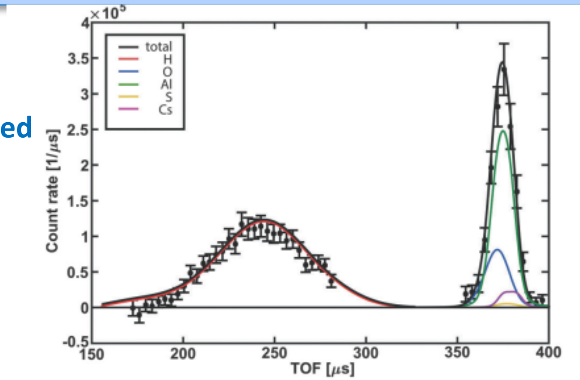

Fig. 8 MANSE data and associated CAAD fits for $CsHSO_4$ phase III at 10 K. For further details, see the main text.

“Atomic and vibrational origins of mechanical toughness in bioactive cement during setting”, K. V. Tian et al., Nature Comm. (2015)- **VESUVIO**

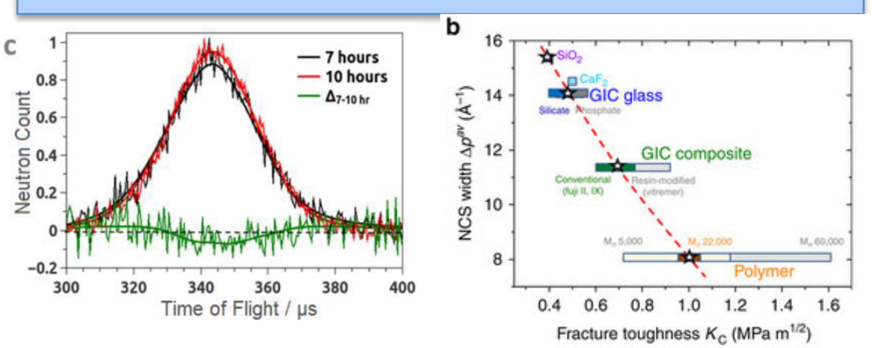

Disordered materials for Dentistry and Health

VESUVIO is now aiming at exploiting element-specific and mass resolved spectroscopy for complex and disordered materials

For a recent overview and discussion please download (FOR FREE): **JOURNAL OF PHYSICS: CONFERENCE SERIES VOLUME 571 (2014). doi:10.1088/1742-6596/571/1/011001**

APPLIED PHYSICS LETTERS **92**, 114101 (2008)

Facility for fast neutron irradiation tests of electronics at the ISIS spallation neutron source

C. Andreani,[1] A. Pietropaolo,[1,a)] A. Salsano,[1] G. Gorini,[2] M. Tardocchi,[2] A. Paccagnella,[3] S. Gerardin,[3] C. D. Frost,[4] S. Ansell,[4] and S. P. Platt[5]
[1]*Centro NAST, Università degli Studi di Roma Tor Vergata, Italy*
[2]*Dipartimento di Fisica "G. Occhialini," Università degli Studi di Milano-Bicocca, Italy*
[3]*Dipartimento di Ingegneria dell'Informazione, Università di Padova, Italy*
[4]*ISIS Facility, Rutherford Appleton Laboratory, Chilton, Didcot, Oxfordshire OX11 0QX, United Kingdom*
[5]*School of Computing, Engineering and Physical Sciences, University of Central Lancashire, Preston, Lancs. PR1 2HE, United Kingdom*

(Received 22 January 2008; accepted 25 February 2008; published online 20 March 2008)

The VESUVIO beam line at the ISIS spallation neutron source was set up for neutron irradiation tests in the neutron energy range above 10 MeV. The neutron flux and energy spectrum were shown, in benchmark activation measurements, to provide a neutron spectrum similar to the ambient one at sea level, but with an enhancement in intensity of a factor of 10^7. Such conditions are suitable for accelerated testing of electronic components, as was demonstrated here by measurements of soft error rates in recent technology field programable gate arrays. © *2008 American Institute of Physics*. [DOI: 10.1063/1.2897309]

from eV to MeV

-Within Italy- UK collaboration on instrumentats for eV-to-MeV neutrons, the Italian team proposed in 2006 a test experiment for irradiation of electronic chips on VESUVIO

-This paved the way to the construction of ChipIr

- The user programme on irradiation continued on VESUVIO and will move to ChipIr

FPR SONS

SoNS

SCHOOL OF NEUTRON SCATTERING
FRANCESCO PAOLO RICCI

2004-Palau: Small Angle (SANS) and Ultra Small Angle (USANS) Scattering
R. Triolo, F. Aliotta

2006-Pula: Structure and Dynamics of Magnetic Systems
P. G. Radaelli, D. Gatteschi

2008-Pula: Near and Intermediate Range Order in Liquids and Soft Matter
M. A. Ricci, M. Zoppi

2010- Frascati: Electron-volt neutron spectroscopy of materials
R. Senesi, C. Vasi

2012- Taormina: Neutron Investigation of Biosystems
C. Andreani, S. Magazù

2014- Erice: Introduction to the theory and techniques of neutron scattering and applications to Cultural Heritage
I. A. Anderson, G. Salvato, A. Scherillo

2015- Erice: ERICE School "NEUTRON SCIENCE AND INSTRUMENTATION": Instruments and devices for neutron scattering experiments
K. H. Andersen, R. Caciuffo

2016- Erice: ERICE School "NEUTRON SCIENCE AND INSTRUMENTATION": Designing and building a neutron instrument
K. H. Andersen, K. W. Herwig

- More than 200 students
- Lecture notes available on website
- multimedia

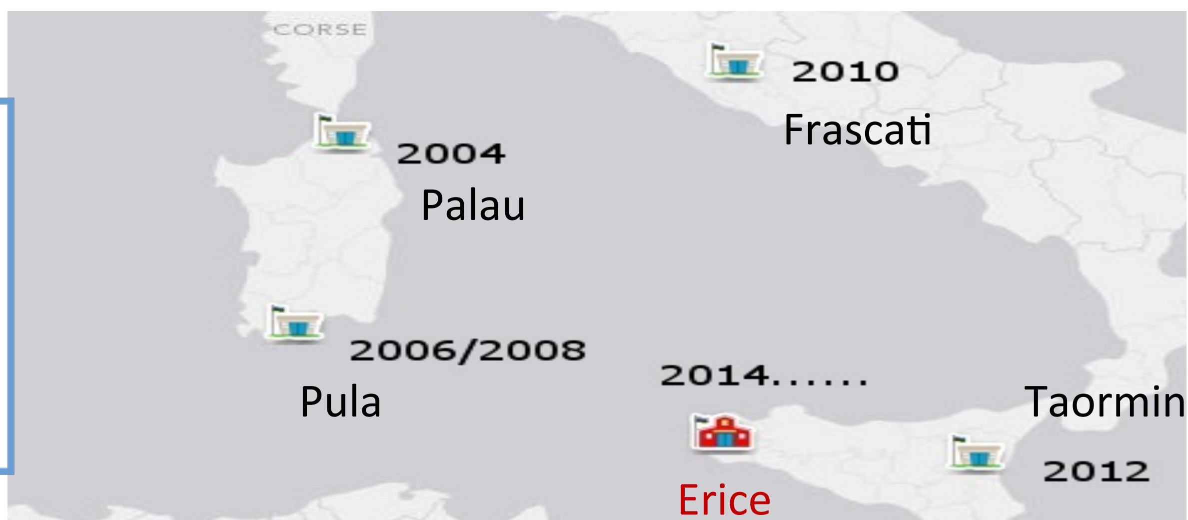

- From 2014: at the Ettore Majorana Foundation and Centre for Scientific Culture
I. A. Anderson
C. Andreani
R. Caciuffo